# Chp 5: The Hydrodynamical Riemann Problem

By

Prof. Dinshaw S. Balsara

# 5.1) Introduction

In Chapter 3 we realized that *non-linear hybridization* introduced by TVD limiters could help us get second order schemes for advection.

We saw in Chapter 4 that even the simplest non-linear hyperbolic cons. law, $u_t + (u^2/2)_x = 0$ can give rise to complex flow features such as *shocks and rarefactions*.

In Chapter 4 we even designed an *approximate Riemann solver* based on the HLL flux for scalar hyperbolic equations. Such a strategy for obtaining a physically sound flux can indeed be extended to hyperbolic systems of conservation laws to yield a basic second order accurate scheme.

But it behooves us to invest a little time to understand strategies for obtaining ***a good, high-quality, physically consistent, properly upwinded numerical flux at the zone boundaries for use in numerical schemes***.

In this chapter we *restrict attention to the Euler equations*. However, the ensuing chapter will show that the insights gained here are of great importance in designing good strategies for obtaining the flux at zone boundaries in numerical schemes for several hyperbolic equations.

Thus imagine that we have a *mesh with fluid variables* defined at the zone centers. We can use our *slope limiters* to endow each flow variable in each zone with a *linear profile*.

As a result, for each zone boundary on a mesh for which we have carried out TVD interpolation of the flow variables, we can obtain the *flow variables to the left and right of any given zone boundary*.

Call the variables to the left of a certain zone boundary ($\rho_{1L}$, $v_{x1L}$, $v_{y1L}$, $v_{z1L}$, $P_{1L}$) and call the corresponding flow variables to the right of the same zone boundary ($\rho_{1R}$, $v_{x1R}$, $v_{y1R}$, $v_{z1R}$, $P_{1R}$) . We want to compute out a set or flow variables at the zone boundary from which we can evaluate the ***numerical flux***. *But how do we obtain this* ***resolved state****?*

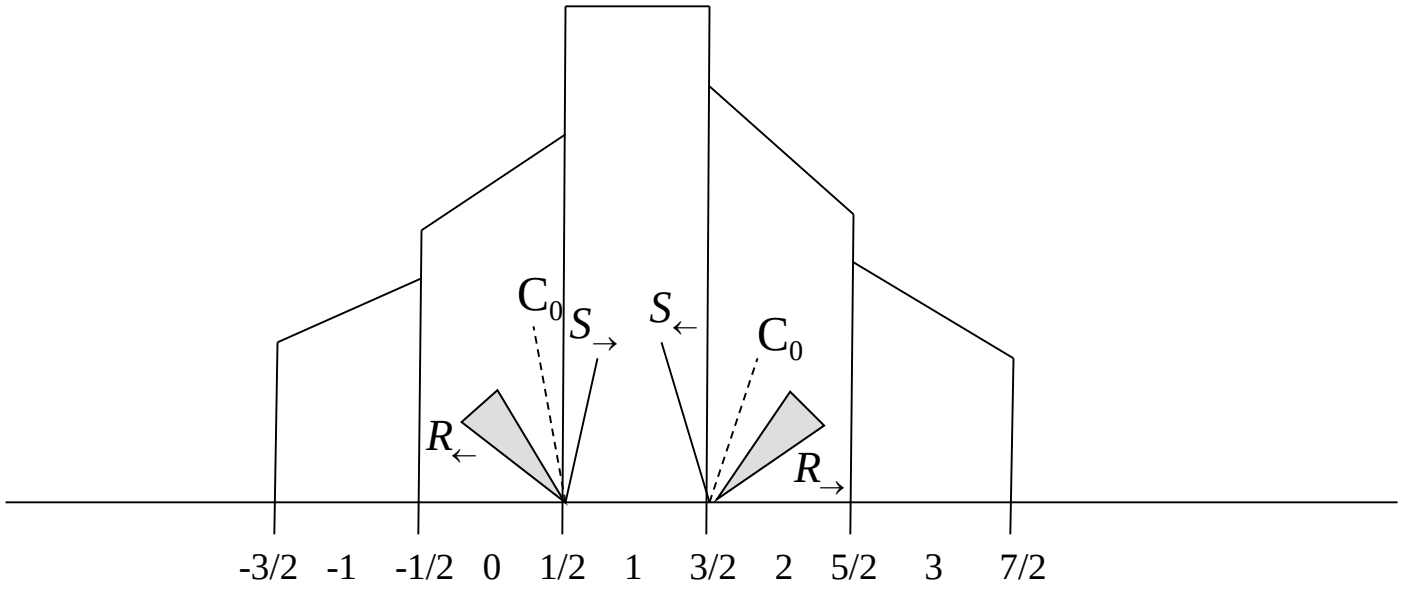

Instinctively, one might want to derive a resolved state by taking an *arithmetic average* of the left and right variables above. If the jump in flow variables is small, the above choice of an arithmetic average might even be adequate. For reasonably small jumps in flow variables, one might even imagine the fluctuations in the flow variables propagating along the characteristics of the flow, as shown in Chp. 1.

However, we know from our study of the Burgers' equation that this choice of resolved state from which to compute a numerical flux would yield *unphysical solutions* even for the simplest of cases when discontinuities are present in the flow.

In general however, the *jump* in densities $\rho_{1L} - \rho_{1R}$ , velocities $v_{x1L} - v_{x1R}$ and pressures $P_{1L} - P_{1R}$ *can be very large* if the flow has a shock.

Early insight on this problem was obtained by ***Bernhardt Riemann*** who analyzed the problem of how flows develop when we have two adjacent slabs of fluid with a discontinuity in flow variables across them.

A mechanical instantiation of the problem considered by Riemann consists of a *shock tube*. Such shock tubes are routinely used to study flows with shocks and the physics of shock waves. A shock tube consists of a long slender tube with a diaphragm in the middle. Initially, the volume to the left of the diaphragm is filled with gas having density and pressure $\rho_{1L}$ and $P_{1L}$ respectively while the right of the gas is filled with gas having density and pressure $\rho_{1R}$ and $P_{1R}$ respectively. At some point, the diaphragm is suddenly removed and we want to know the subsequent flow features that develop in the tube. A schematic fig. is provided below

We readily see that, but for permitting arbitrary velocities $v_{x1L}$ and $v_{x1R}$ to the left and right, the problem that interested Riemann is very similar to the problem that interests us. We call the problem of determining the resolved state arising from such discontinuous initial conditions the ***Riemann Problem*** in honor of Riemann.

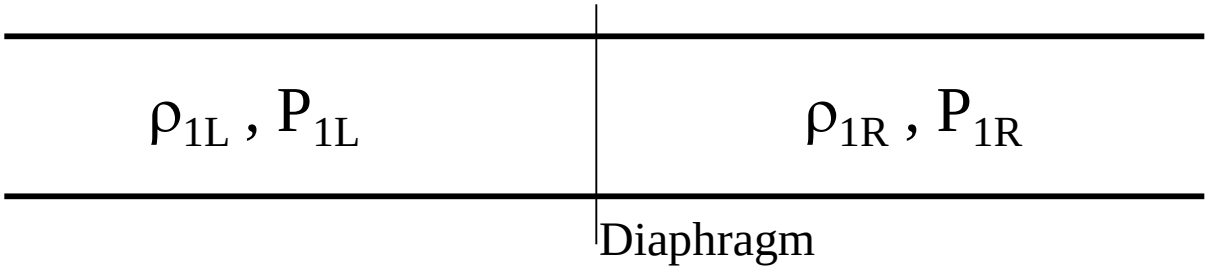

Riemann's ingenious realization was that even though the problem involved strong jumps in density, pressure and possibly velocity, the resolution of the discontinuity would *bear some imprint of the linearized problem with some important differences*!

From Chp. 1 we already know that the ***linearized problem*** with very small fluctuations (i.e. say a very small jump in flow variables across the diaphragm) that are localized at a point along the x-axis would resolve itself into:

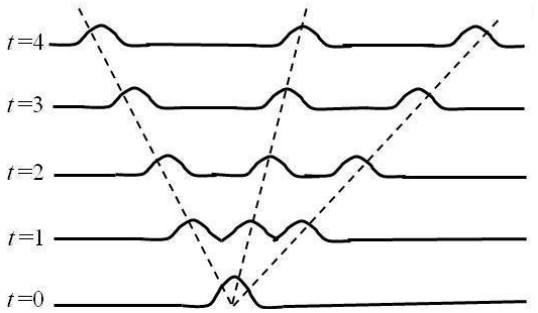


**i)** *a right-going sound wave*,
**ii)** *a left-going sound wave*
**iii)** *an entropy wave* between them.

The entropy wave may well have an additional shear across it. The shear is brought on by the fact that $v_{y1L}$ may differ from $v_{y1R}$ and similarly for $v_{z1L}$ and $v_{z1R}$ .

Question: Can you recall the properties of scalar conservation laws with convex fluxes?

Riemann realized that the ***fully non-linear problem*** (i.e. with arbitrary jumps in flow variables across the diaphragm) would resolve itself into:

**i)** *a right-going shock wave or rarefaction fan*,
**ii)** *a left-going shock wave or rarefaction fan*
**iii)** *an entropy pulse* which may well have an additional shear in the transverse velocities.

The connection between the linearized problem and the fully non-linear problem can be made very concrete by realizing that :

**i)** a finite amplitude right-going sound wave can self-steepen into a right-going shock or open out to become a right-going rarefaction wave,

**ii)** finite amplitude left-going sound wave can self-steepen into a left-going shock or open out into a left-going rarefaction wave,

**iii)** an entropy wave, being linearly degenerate, can have any entropy jump across it. When the entropy jump across an entropy wave becomes large, the wave becomes an entropy pulse.

A schematic representation in the x-t plane of a Riemann problem with a right-going shock, a left-going rarefaction fan and a contact discontinuity between the two is shown below. (An entropy pulse is also often referred to as a *contact discontinuity*.)

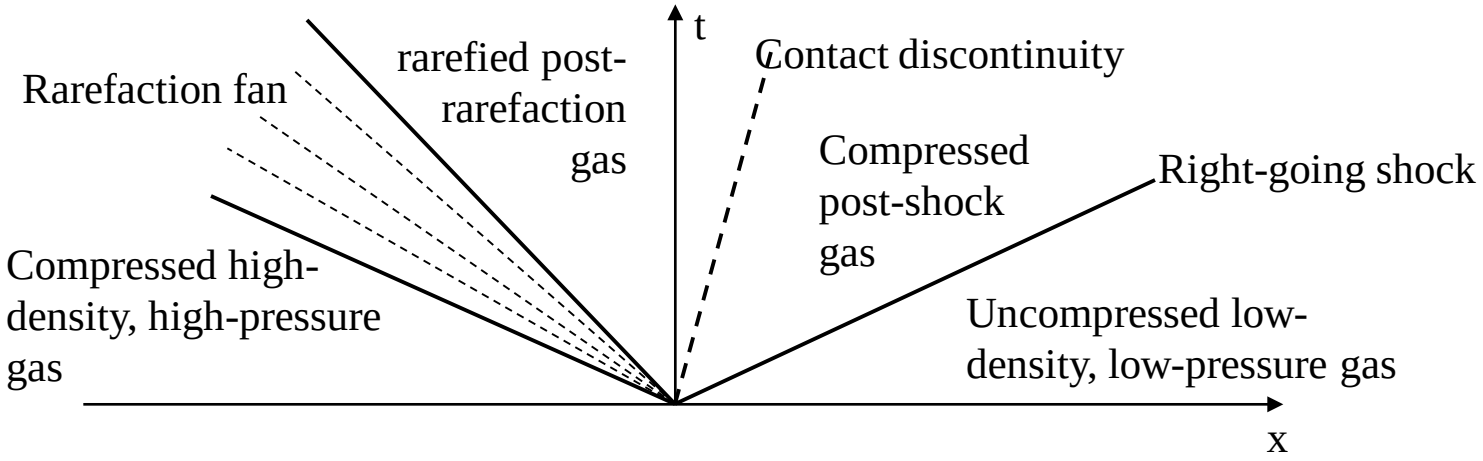

# 5.1.2) Introducing the Riemann Problem as a Building Block for Numerical Schemes

Godunov (1959) viewed flow variables in each zone of a mesh as being slabs of fluid. The slabs would obviously have discontinuities between them at the zone boundaries. Godunov suggested that the *Riemann problem* be used to obtain a resolved state at each zone boundary. His important insight was that *fluid fluxes* computed with that resolved state would naturally be *physically consistent and properly upwinded*!

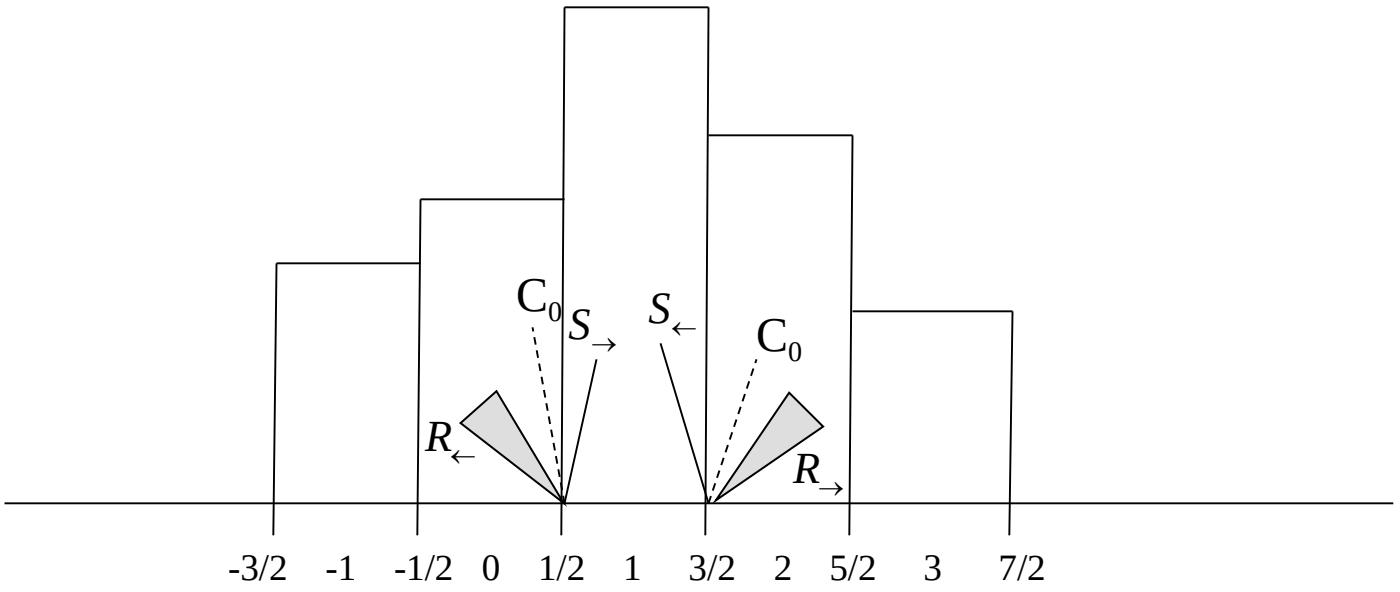

A schematic of Godunov's method is shown above. It can be broken up into the two following conceptual steps:
**i)** Discretize the Conservation law, $U_t + F(U)_x = 0$ , as slabs of fluid.
**ii)** Solve the Riemann problems at zone boundaries, get fluxes and update.

Godunov's method was slow in taking off. In truth, the Riemann problem had to be solved iteratively and the iterative method proposed by Godunov was slow to converge. This made the scheme slower than other competitive schemes from that era.
Furthermore, the method was only first order accurate making it very dissipative.

In a tour de force, van Leer (1979) proposed a second order extension of Godunov's scheme. van Leer's paper has been cited thousands of times.

van Leer proposed the following *cutting-edge advances* all at once:
**i)** A very efficient *iterative solution strategy to the Riemann problem* which is still used mostly without change.
**ii)** A strategy for using *piecewise-linear monotonicity preserving reconstruction* of the sort studied in the previous chapter. This made the scheme spatially second order accurate while enabling shock capturing.
**iii)** A method for *increasing the temporal accuracy to second order*. van Leer later realized that this could also be achieved by using the Runge-Kutta time-stepping that was catalogued in Chp. 3.

***van Leer's scheme***, with several modifications, is still used as a blueprint for several successful numerical codes. A possible variant of his scheme can be described schematically by the following three steps:
**i)** Use a *second-order Runge-Kutta scheme* to achieve second order accuracy in time. Each of the stages in the two-stage scheme consists of the following two steps.
**ii)** Make *piecewise linear profiles* within each zone for the density, pressure and velocity. Do this using the limiters described in Chp. 3. This gives the scheme second order accuracy in space.

**iii)** Compute the *fluxes using the Riemann solver* described in this chapter and finite difference the fluxes to obtain the time rates of update, i.e. $U_t = - F(U)_x$ , that are needed in the Runge-Kutta scheme.

van Leer's scheme is shown schematically below. By the end of this chapter the reader should be able to construct a similar flow solver using the codes provided in this book.

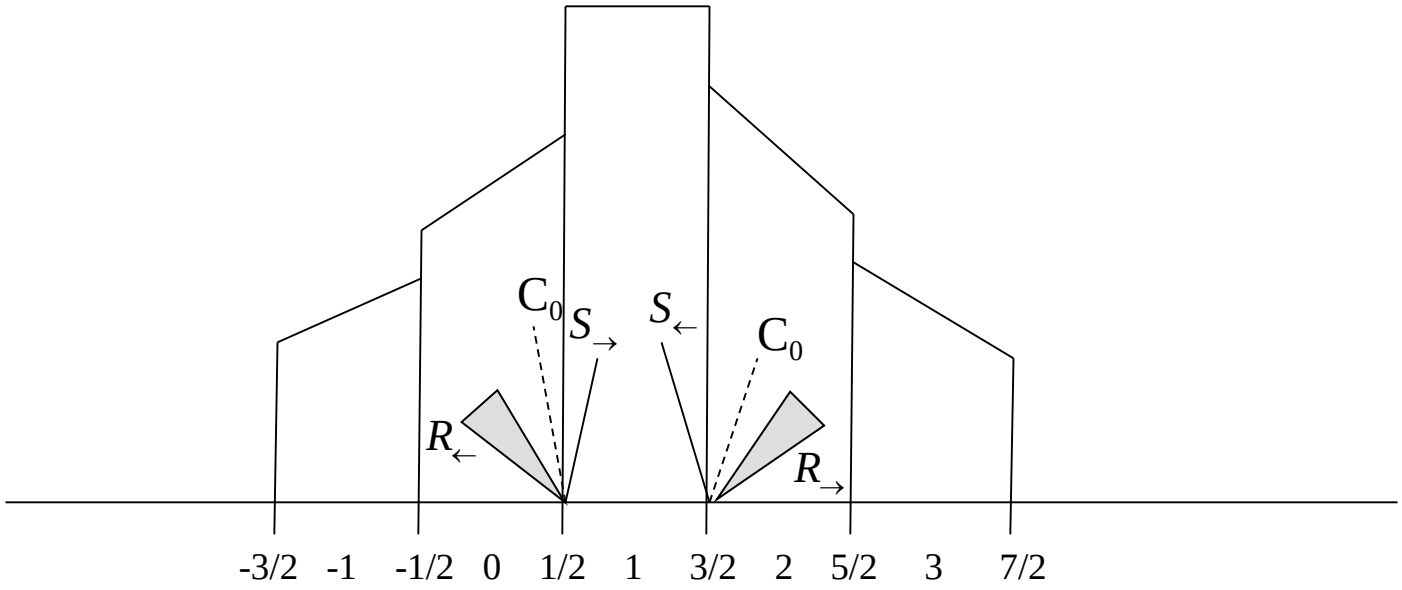

# 5.2) Hydrodynamical Shock Waves

## 5.2.1) Shock Jump Conditions

Our equation for the jumps across a shock is given by : $f(u_r) - f(u_l) = s(u_r - u_l)$

While the above was derived for a scalar, non-linear hyperbolic equation, it is easy to see that the construction is quite general. In particular, it can be applied without change to each of the the components of a hyperbolic system of conservation laws.

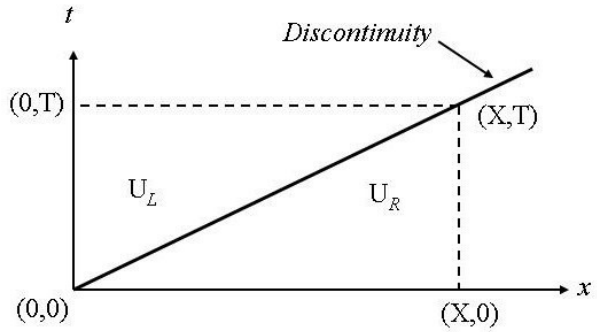


The bulk of insight can be gained by considering the one-dimensional Euler system written in conservation form.

$$\frac{\partial}{\partial t}\begin{pmatrix}\rho\\ \rho v_x\\ \rho v_y\\ \rho v_z\\ \varepsilon\end{pmatrix} + \frac{\partial}{\partial x}\begin{pmatrix}\rho v_x\\ \rho v_x^2 + P\\ \rho v_x v_y\\ \rho v_x v_z\\ (\varepsilon + P) v_x\end{pmatrix} = 0 \; ; \quad \varepsilon = \rho\left(\frac{1}{2}\vec{v}^{\,2} + \frac{1}{\Gamma - 1}\frac{P}{\rho}\right) \text{ for polytropic gas}$$

$$\frac{\partial}{\partial t}\begin{pmatrix} \rho \\ \rho\, v_x \\ \rho\, v_y \\ \rho\, v_z \\ \varepsilon \end{pmatrix} + \frac{\partial}{\partial x}\begin{pmatrix} \rho\, v_x \\ \rho\, v_x^2 + P \\ \rho\, v_x\, v_y \\ \rho\, v_x\, v_z \\ (\varepsilon + P)\, v_x \end{pmatrix} = 0 \; ; \quad \varepsilon = \rho \left( \frac{1}{2} \vec{v}^{\,2} + \frac{1}{\Gamma - 1} \frac{P}{\rho} \right) \; ; \quad h \equiv \frac{e + P}{\rho} = \frac{\Gamma}{\Gamma - 1} \frac{P}{\rho}$$

It is just plain easier to work in the rest frame of the discontinuity .

In that frame we can set the speed of the discontinuity to zero, i.e. s = 0.

Since the Euler equations are Galilean invariant, this is tantamount to picking a favorable frame of reference in which the problem simplifies. Denote velocity variables in that frame to be "**u**", instead of "**v**".

## Jump Conditions Across **Any** Discontinuity:

We denote the pre-shock and post-shock parts of the discontinuity by subscripts "1" and "2" respectively. Thus in the frame of the discontinuity, where the velocity is called "u", we get a set of balance conditions for the fluid fluxes:

Balancing mass flux : $\left[\rho\, u_x\right] = 0 \Rightarrow \rho_1\, u_{x1} = \rho_2\, u_{x2}$

Balancing x-momentum flux : $\left[\rho\, u_x^2 + P\right] = 0 \Rightarrow \left(\rho_1\, u_{x1}^2 + P_1\right) = \left(\rho_2\, u_{x2}^2 + P_2\right)$

Balancing y-momentum flux : $\left[\rho\, u_x\, u_y\right] = 0 \Rightarrow \rho_1\, u_{x1}\, u_{y1} = \rho_2\, u_{x2}\, u_{y2}$

Balancing z-momentum flux : $\left[\rho\, u_x\, u_z\right] = 0 \Rightarrow \rho_1\, u_{x1}\, u_{z1} = \rho_2\, u_{x2}\, u_{z2}$

Balancing energy flux: $\Rightarrow \rho_1\, u_{x1} \left(\frac{1}{2}\, \mathbf{u}_1^2 + h_1\right) = \rho_2\, u_{x2} \left(\frac{1}{2}\, \mathbf{u}_2^2 + h_2\right)$

Equation of State: $h \equiv \frac{e + P}{\rho}$ and specific enthalpy $h = \frac{\Gamma}{\Gamma - 1}\, \frac{P}{\rho}$ for polytropic gas.

The first natural solution may well be to set the mass flux across the discontinuity to zero: $\rho_1 \, u_{x1} = \rho_2 \, u_{x2} = 0$ . Notice $\rho_1 \neq 0$ and $\rho_2 \neq 0$. Notice too that we do not require $\rho_1$ and $\rho_2$ to equal eachother.

This gives us : $u_{x1} = u_{x2} = 0$ ; $[P] = 0$ ; $[u_y] = anything$ ; $[u_z] = anything$

Question: What does this really mean? Question: In an eigenmodal analysis, which waves would this correspond to and why? Question: If such a discontinuity indeed had a finite jump in $u_y$ or $u_z$ , would it be stable? What's it called?

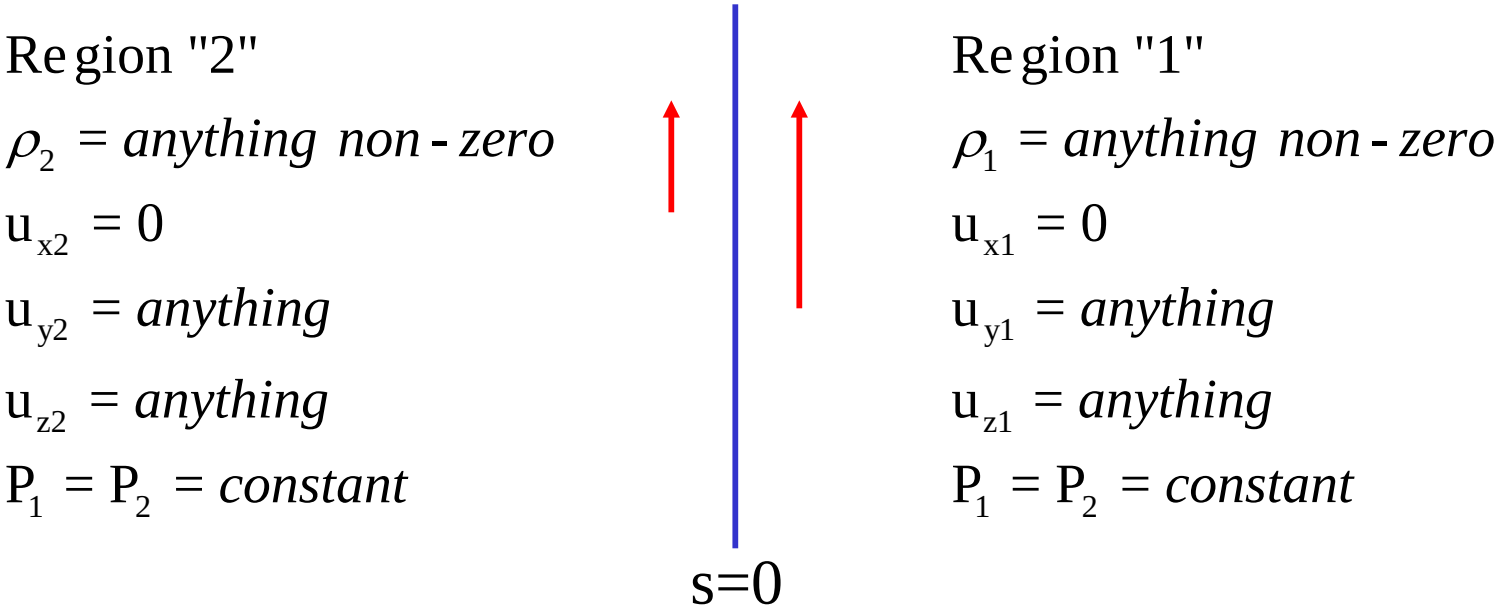

# Linearly Degenerate waves for The Euler and the MHD equations

Typically, the contact discontinuity that arises for the Euler equations can also have an associated shear wave. This is symptomatic of the fact that the eigenvectors with $\lambda = v_x$ in the Euler system permit an *entropy wave* (with any possible jump in entropy) as well as *shear waves* (with any possible jump in velocity shear), all with the same eigenvalue. Such waves do not steepen as they propagate in space. They are, therefore, known as *linearly degenerate waves* as opposed to *genuinely non-linear waves* , i.e. the *sound waves*, which do steepen as they propagate.

The MHD equations also sustain an entropy wave. If the magnetic field is non-zero in the direction of wave propagation, then such an entropy wave *cannot sustain a shear* in the transverse velocities across it. This is because the magnetic field breaks the degeneracy of eigenvalues noted above. Now it is the *torsional Alfven waves that carry the shear* in the flow. The MHD system then has one entropy wave and two Alfven waves as its linearly degenerate waves while the magnetosonic waves are nonlinear. The *fast magnetosonic wave* then serves as the precise analogue of sound waves.

Now let us consider discontinuities where there is a non-zero mass flux:

i.e. $\rho_1 \, u_{x1} = \rho_2 \, u_{x2} \neq 0$.

The y- and z-momentum balance conditions immediately give us:

$\left[ u_y \right] = 0$ ; $\left[ u_z \right] = 0$ . Question: What does this mean physically?

To have a non-trivial discontinuity, we need $\rho_1 \neq \rho_2$ and $u_{x1} \neq u_{x2}$ .

Question: Right-going shock shown below. What changes in a left-going shock?

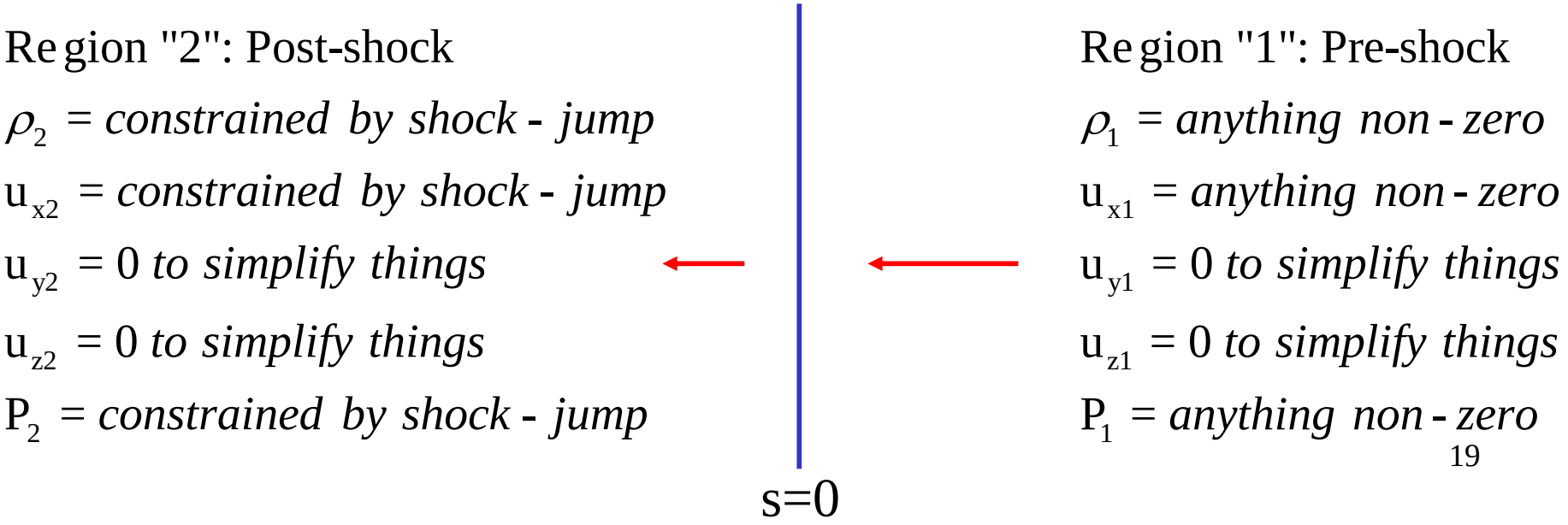

Balancing mass flux : $\left[\rho\, u_x\right] = 0 \Rightarrow \rho_1\, u_{x1} = \rho_2\, u_{x2}$

Balancing x-momentum flux : $\left[\rho\, u_x^2 + P\right] = 0 \Rightarrow \left(\rho_1\, u_{x1}^2 + P_1\right) = \left(\rho_2\, u_{x2}^2 + P_2\right)$

Balancing y-momentum flux : $\left[\rho\, u_x\, u_y\right] = 0 \Rightarrow \rho_1\, u_{x1}\, u_{y1} = \rho_2\, u_{x2}\, u_{y2}$

Balancing z-momentum flux : $\left[\rho\, u_x\, u_z\right] = 0 \Rightarrow \rho_1\, u_{x1}\, u_{z1} = \rho_2\, u_{x2}\, u_{z2}$

Balancing energy flux: $\Rightarrow \rho_1\, u_{x1} \left(\frac{1}{2}\, \mathbf{u}_1^2 + h_1\right) = \rho_2\, u_{x2} \left(\frac{1}{2}\, \mathbf{u}_2^2 + h_2\right)$

$$\left[\rho\, u_x\right] = 0 \quad ; \quad \left[\rho\, u_x^2 + P\right] = 0 \quad ; \quad \left[\frac{1}{2}\, u_x^2 + h\right] = 0$$

The mass momentum and energy balance conditions for this type of discontinuity then simplify to:

$$\left[\rho\, u_x\right] = 0 \quad ; \quad \left[\rho\, u_x^2 + P\right] = 0 \quad ; \quad \left[\frac{1}{2}\, u_x^2 + h\right] = 0$$

This type of discontinuity is known as a **shock wave**. The above balance conditions are also known as *shock jump conditions* or *Rankine - Hugoniot jump conditions*. Since shocks emerge through self-steepening of sound waves, it is natural to think of shocks as the non-linear extension of sound waves. As a result, for one-dimensional flow we have left and right-going shocks.

A physical shock should also raise the entropy of the fluid that flows through it. Thus we expect the post-shock temperature and density to be higher than the pre-shock values. On intuitive grounds we thus expect that a **right - going shock** in one-dimension has : $\rho_2 > \rho_1$ ; $P_2 > P_1$ ; $T_2 > T_1$ and, therefore in the shock's rest frame we have $u_{x1} < 0$ and $u_{x2} < 0$ and $|u_{x2}| < |u_{x1}|$.

Question: Can you specify the similar conditions for a left-going shock?

For the Burgers equation $u_t + \left(u^2/2\right)_x = 0$ we saw that there is only one family of characteristics and that they converge at a shock. A similar trend prevails for systems of hyperbolic equations where the *shock is the locus formed by converging characteristics of a given wave family*.

Thus notice that the family of $C_+$ characteristics formed by $\lambda = v_x + c_s$ on either side of a right-going shock actually flow into such a shock. This becomes evident once one realizes that the self-steepening of right-going sound waves is one of the ways one can form a right-going shock. Similarly, a left-going shock is the locus of converging $C_-$ characteristics formed by $\lambda = v_x - c_s$.

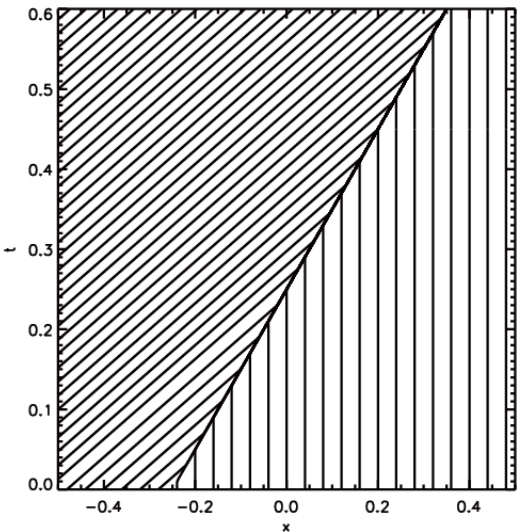


Question: Recall the Lax entropy condition. What does it say for the characteristics on either side of a shock wave?

To figure out which direction a one-dimensional shock is headed, "*follow the entropy*". Physically consistent shock waves always raise the entropy in the post-shock region. The pre-shock fluid is the low entropy fluid that has not yet been run over by a shock. The post-shock fluid is the high entropy fluid that has had its entropy raised by passage through a shock. Within the shock, the viscous terms are very important in raising the entropy of the shock.

Question: What does the entropy condition imply for the characteristics? How do they flow relative to a shock?

The viscosity operates in a thin layer around the shock and numerical schemes for shock-capturing often try to reproduce the same physical process by including some amount of artificial viscosity. But watch out for astrophysical shocks which can often be collisionless shocks. Question: How do such shocks "thermalize" the velocity distribution in their atoms?

Consider a flow with v ~ $c_s$ taking place in a system of size "L". The viscosity is $\eta$ (where $\eta$ ~ $c_s$ $l$) and $l$ is the mean free path in the gas. Then Re ~ v L / $\eta$ ~ (v L)/($c_s$ $l$) . Far from the shock, the length scales L that govern the sytem are much larger than $l$ so that Re >> 1 and viscous terms are unimportant. Close to the shock, the characteristic length of the system is the thickness of the shock so L ~ $l$ and so Re ~ 1. This shows that the viscous stresses are very important in modulating the shock jump though they are unimportant elsewhere.

Strong shocks have larger jumps in their variables. As a result, the viscous terms can operate more efficiently at stronger shocks with the result that stronger shocks have a smaller viscous width than weaker shocks.

We now intuit that the strength of a shock might depend on the extent to which the entropy is raised across a shock. This is absolutely correct. In fact, any other physical tracer of an entropy increase, like an increase in pressure or temperature will do.

## 5.2.2) The Hugoniot Adiabat

Given a specification of the pre-shock density and pressure and a *single parameter measuring the shock strength, say the post-shock pressure*, we wish to predict the other thermodynamic conditions in the post-shock region.

The *Hugoniot adiabat* permits us to do just that. Question: What is an adiabat?

I.e., we are expressing the intuition that for a given set of pre-shock thermodynamic variables and *one* post-shock variable, we should be able to find *all the other* thermodynamic variables as a one-parameter sequence.

To arrive at a condition like this, we realize that we might want to eliminate the velocities. Also realize that $u_y$ and $u_z$ are constant across a normal shock so we can simplify by setting $u_y = u_z = 0$.

The equations also work out more simply if we use the *specific volumes*: $V_1 = 1/\rho_1$ and $V_2 = 1/\rho_2$ .

Mass Balance: $\rho_1 \, u_{x1} = \rho_2 \, u_{x2} \equiv j \;\Rightarrow\; u_{x1} = j\,V_1 \; ; \; u_{x2} = j\,V_2$

Momentum Balance: $\rho_1 \, u_{x1}^2 + P_1 = \rho_2 \, u_{x2}^2 + P_2 \;\Rightarrow\; j^2 \, V_1 + P_1 = j^2 \, V_2 + P_2$

$\Rightarrow \; j^2 = \dfrac{P_2 - P_1}{V_1 - V_2}$ $\leftarrow$ "j" is called the mass flux variable.

Because $j^2$ is positive, we can only have two mathematically consistent situations : 1) $P_2 > P_1$ and $V_1 > V_2 \left(\Leftrightarrow \rho_2 > \rho_1\right)$ or 2) $P_2 < P_1$ and $V_1 < V_2$ . By convention we take "1" to be the pre-shock gas. As a result, only the former is *physically consistent* with entropy generation at the shock.

Question : We get $j = \mp \sqrt{\dfrac{P_2 - P_1}{V_1 - V_2}}$ ; what do each of the signs correspond to?

Energy Balance: $h_1 + \frac{1}{2}u_{x1}^2 = h_2 + \frac{1}{2}u_{x2}^2 \Rightarrow h_1 + \frac{1}{2}j^2 V_1^2 = h_2 + \frac{1}{2}j^2 V_2^2$

$$\Rightarrow \quad \boxed{h_1 - h_2 + \frac{1}{2}(V_1 + V_2)(P_2 - P_1) = 0} \leftarrow \text{Hugoniot adiabat}$$

We can even write it in terms of the specific internal energy by setting $h = e\,V + P\,V$ to get:

$$\Rightarrow \; e_1 V_1 - e_2 V_2 + \frac{1}{2}(V_1 - V_2)(P_2 + P_1) = 0 \quad \leftarrow \text{Hugoniot adiabat}$$

For most real gases, $\Gamma$ is a slowly varying parameter. As a result, we can freeze it around some local value as was shown in the design of the Riemann problem for real gases in Colella & Glaz (1994). To solve for the shock structure we can make local iterations around the shock state to find an approximate value of $\Gamma$ .

We will study the Riemann problem in time. For that problem, it is *very useful to have a compact* exp*ression for* $u_{x1} - u_{x2}$ . To do this, first obtain $u_{x1} - u_{x2} = j\,(V_1 - V_2)$ and then use $j^2 = (P_2 - P_1)/(V_1 - V_2)$ to get:

$$u_{x2} - u_{x1} = \pm\sqrt{(P_2 - P_1)(V_1 - V_2)}$$

We will show very shortly in the next section that $u_{x2} - u_{x1} > 0$ for right-going shocks and $u_{x2} - u_{x1} < 0$ for left-going shocks. Note too that for a shock we will always have $P_2 > P_1$ and $\rho_2 > \rho_1$ or $V_2 < V_1$ .



Notice that all the eqns in this section are independent of EOS.

# 5.2.3) Normal Shocks in Polytropic Gases

Many of the requisite insights in computational science and engineering can be gained by studying normal shocks. We do that here.

Even when gases are not polytropic, like in the interior of a pre-supernova star, they behave somewhat like polytropic gases in restricted density and temperature ranges. Besides, the plasma in several problems can indeed be treated as polytropic to a very good approximation.

Using the polytropic relation $\left( h = \frac{\Gamma}{\Gamma - 1} \frac{P}{\rho} \right)$ in the previous Hugoniot adiabat, show that the following condition holds:

$$\frac{\rho_1}{\rho_2} = \frac{u_{x2}}{u_{x1}} = \frac{V_2}{V_1} = \frac{(\Gamma+1)\, P_1 + (\Gamma-1)\, P_2}{(\Gamma-1)\, P_1 + (\Gamma+1)\, P_2}$$

We can now plot out the Hugoniot adiabat for a polytropic gas, done below.

Question: In the limit $\frac{P_2}{P_1} \rightarrow \infty$, what is $\frac{\rho_2}{\rho_1}$ ? Why do we not care for the limit $\frac{P_2}{P_1} \rightarrow 0$ ? ( Assume that subscript "1" denotes pre-shock gas.)

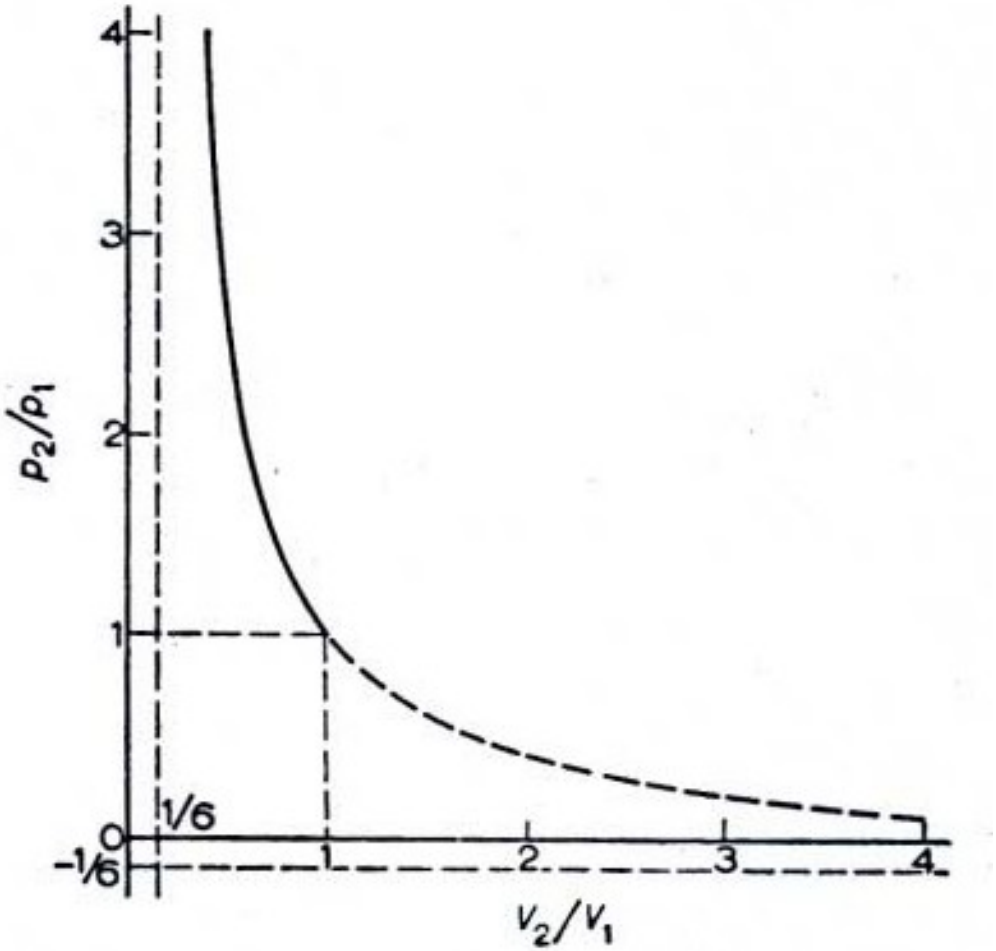

Using $T_2 / T_1 = (P_2\ V_2) / (P_1\ V_1)$ and the previous eqn. we can show that:

$$\frac{T_2}{T_1} = \frac{P_2}{P_1}\ \frac{(\Gamma+1)\ P_1 + (\Gamma-1)\ P_2}{(\Gamma-1)\ P_1 + (\Gamma+1)\ P_2}$$

Furthermore, we can use the relation $j^2 = (P_2 - P_1)/(V_1 - V_2)$ along with the next to previous eqn. to show that:

$$j^2 = \left[(\Gamma-1)\ P_1 + (\Gamma+1)\ P_2\right] / (2\ V_1)$$

Use $u_{x1} = j\, V_1$ and the results from the previous eqn. to obtain:

$$u_{x1}^2 = \frac{1}{2} V_1 \left[ (\Gamma - 1) P_1 + (\Gamma + 1) P_2 \right] = \frac{1}{2} \left( c_{s1}^2 / \Gamma \right) \left[ \Gamma - 1 + (\Gamma + 1) P_2 / P_1 \right]$$

Now use $u_{x2} = V_2\, u_{x1} / V_1$ and the above result to obtain:

$$u_{x2}^2 = \frac{1}{2} V_1 \left[ (\Gamma + 1) P_1 + (\Gamma - 1) P_2 \right]^2 \Big/ \left[ (\Gamma - 1) P_1 + (\Gamma + 1) P_2 \right]$$

$$= \frac{1}{2} \left( c_{s2}^2 / \Gamma \right) \left[ \Gamma - 1 + (\Gamma + 1) P_1 / P_2 \right]$$

In preparation for our study of the Riemann problem, it is also useful to take the expression for the velocity jump $u_{x1} - u_{x2}$ from the last section and show that:

$$u_{x2} - u_{x1} = \pm \left( P_2 - P_1 \right) \sqrt{\frac{2 V_1}{(\Gamma - 1) P_1 + (\Gamma + 1) P_2}}$$

Where the +ve and –ve signs above are for right- and left-going shocks respectively.

In the previous formulae, we used the pressure ratio, $P_2 / P_1$ , as a measure of the strength of the shock. It sometimes helps to use the pre-shock **Mach number**, $M_1 = u_{x1} / c_{s1}$ , as a measure of the strength of the shock. We wish to derive formulae that depend on $M_1$ because such formulae are often very useful in setting up isolated hydrodynamical shocks. Similar formulae for MHD are given in Jefferey & Taniuti's text.

Use the formula for $u_{x1}^2$ from the penultimate eqn. to express the pressure ratio, $P_2 / P_1$ , in terms of the Mach number $M_1$ as:

$$P_2/P_1 = \left[2\,\Gamma\,M_1^2 - (\Gamma-1)\right]/(\Gamma+1)$$

Put this in our ratio of $V_2 / V_1$ to obtain:

$$\rho_2/\rho_1 = u_{x1}/u_{x2} = (\Gamma+1)\,M_1^2/\left[(\Gamma-1)\,M_1^2 + 2\right]$$

$$T_2/T_1 = \left[2\,\Gamma\,M_1^2 - (\Gamma-1)\right]\left[(\Gamma-1)\,M_1^2 + 2\right]/\left[(\Gamma+1)^2\,M_1^2\right]$$

Equating the pressure ratio, $P_2 / P_1$ , in formulae for $u_{x1}^2$ and $u_{x2}^2$ from the previous eqns gives:

$$M_2^2 = \left[(\Gamma-1)\,M_1^2 + 2\right]/\left[2\,\Gamma\,M_1^2 - (\Gamma-1)\right]$$

These equations clearly show that as $M_1$ increases so that $M_1 \rightarrow \infty$ ,

i.e. as we get progressively stronger shocks, we have:

$$\frac{\rho_2}{\rho_1} \rightarrow \frac{(\Gamma+1)}{(\Gamma-1)} \quad ; \frac{P_2}{P_1} \rightarrow \infty \quad ; \frac{T_2}{T_1} \rightarrow \infty \quad ; \frac{M_2}{M_1} \rightarrow \sqrt{\frac{(\Gamma-1)}{2\Gamma}}$$

These equations are made even more meaningful by the fact that we observe several strong-shock phenomena in high speed flow. Question : Give examples.

Question: For strong shocks that are not infinite shocks can you use the previous examples to show that: $\frac{u_{x1}}{u_{x2}} = \frac{V_1}{V_2} = \frac{\rho_2}{\rho_1} = \frac{(\Gamma+1)}{(\Gamma-1)}$ ; $\frac{T_2}{T_1} = \frac{(\Gamma-1)}{(\Gamma+1)} \frac{P_2}{P_1}$

$$u_{x1} = \sqrt{\frac{(\Gamma+1)\ P_2}{2\ \rho_1}} \quad ; \ u_{x2} = \sqrt{\frac{(\Gamma-1)^2\ P_2}{2\ (\Gamma+1)\ \rho_1}}$$

Notice that the post-shock pressure is always larger than the pre-shock pressure in a hydrodynamical shock. Thus, we say that all hydro shocks are *compressive shocks*, a property shared by MHD shocks.

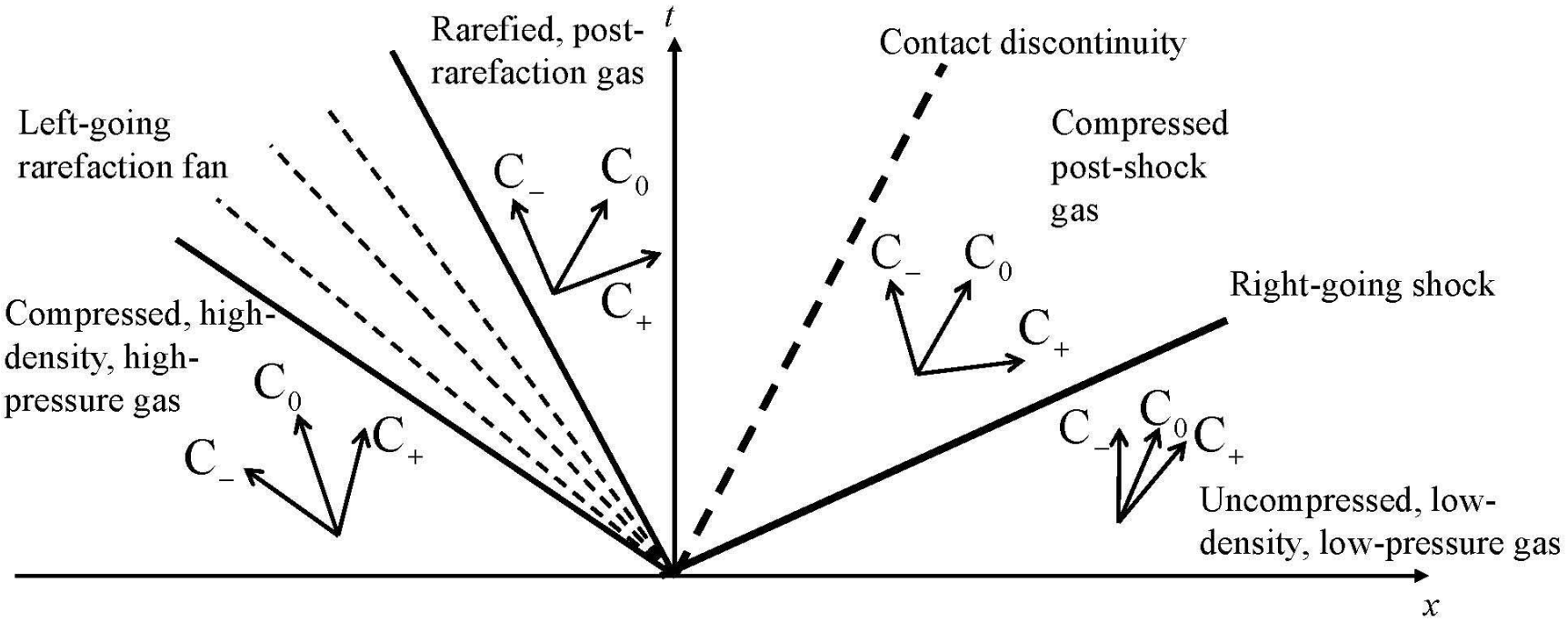


*Schematic space-time diagram of a Riemann problem showing the characteristic speeds in all of the constant states. Notice that the $C_+$ characteristics on either side of the right-going shock propagate into the shock. The $C_0$ characteristics on either side of the contact discontinuity are parallel to it. The $C_-$ characteristics on either side of the left-going rarefaction fan are parallel to the characteristics that bound the fan.*

This figure shows us that the shocks that arise in the Euler equation are all *classical shocks*.

Notice the $C_0$ characteristic families around the contact discontinuity and the rarefaction fan.

# 5.2.4) Shocks in the Lab Frame

Notice that we have zeroed out the transverse velocities and solved the problem in the rest-frame of the discontinuity. In some sense, this is a restriction on the form of the pre-shock velocities. We can go to the more general case by using a Galilean transformation.

Thus say that the pre-shock velocity in any general frame of reference is given by $v_{x1}\ \hat{x} + v_{y1}\ \hat{y} + v_{z1}\ \hat{z}$ . Say the pre-shock pressure and density are $P_1$ and $\rho_1$ respectively and the post-shock pressure is $P_2$, which defines the strength of the shock.

We can use this information to find the velocity $u_{x1}$ of the pre-shock fluid in the shock's rest frame.

Then if we transform from the current coordinate system $\mathbf{F}$ to a frame $\mathbf{F}'$ which is moving with velocity $\mathbf{v}_{\mathbf{F}'} = (v_{x1} - u_{x1})\hat{x} + v_{y1}\,\hat{y} + v_{z1}\,\hat{z}$ with respect to it, we would be in the shock's rest frame.

As seen in the lab frame the shock is moving with the velocity of the frame $\mathbf{F}'$ relative to the reference frame $\mathbf{F}$ .

In the general frame of reference **F**, the post-shock velocity vector should then be $(v_{x1} + u_{x2} - u_{x1})\,\hat{x} + v_{y1}\,\hat{y} + v_{z1}\,\hat{z}$ .

We thus see that if $u_{x2} - u_{x1}$ can be specified as a function of $P_1$ , $\rho_1$ and $P_2$ then we can specify the post-shock velocity $v_{x2}$ exactly.

The velocity jump is unchanged : $v_{x2} - v_{x1} = u_{x2} - u_{x1}$

Right-going shock, Changing the frame of reference:-

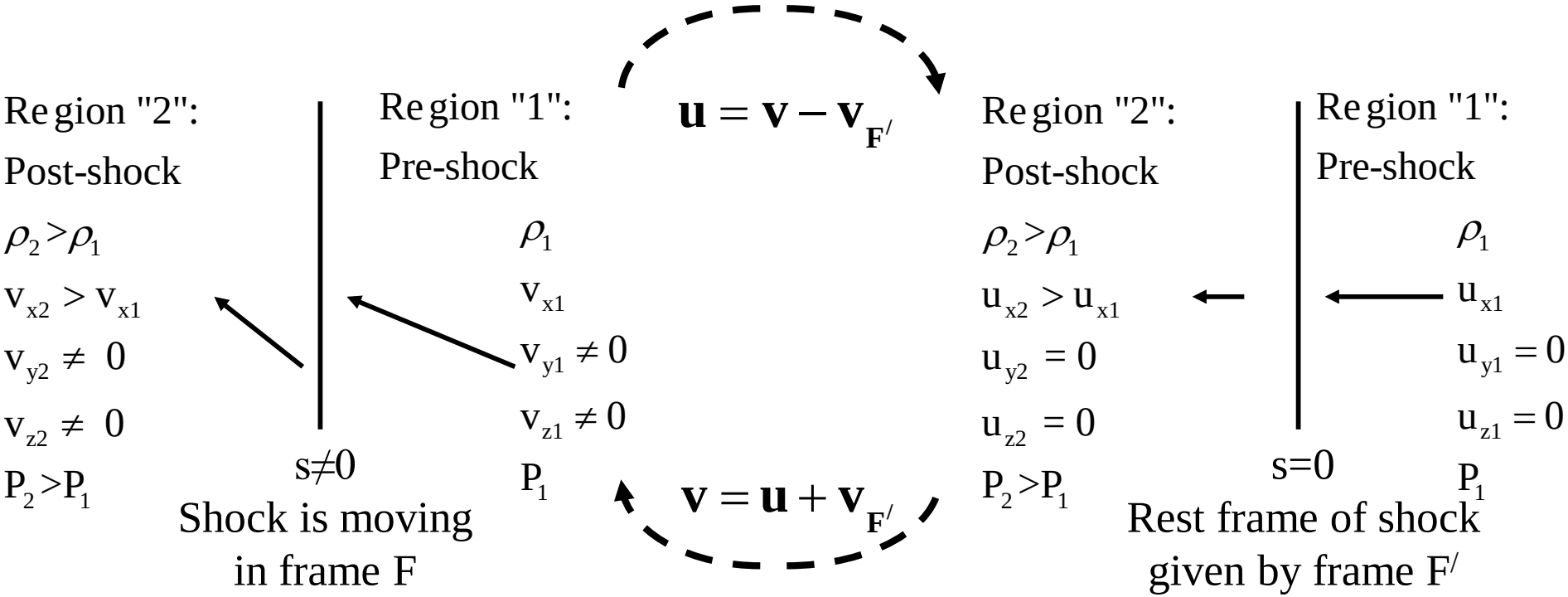


$$\mathbf{v}_{F'} = \left(v_{x1} - u_{x1}\right)\hat{x} + v_{y1}\,\hat{y} + v_{z1}\,\hat{z}$$

For ***right-going shocks*** we then have $v_{x2} = v_{x1} + u_{x2} - u_{x1}$ so that :

$$v_{x2} = v_{x1} + \left(P_2 - P_1\right)\sqrt{\frac{2\,V_1}{\left(\Gamma - 1\right)P_1 + \left(\Gamma + 1\right)P_2}}$$

To see why the shock is right-going, set $v_{x1} = 0$, i.e. the fluid to the right of the shock is not moving. In that case, $v_{x2} > 0$ and the shock overruns the fluid to the right. Since the shock is stationary in its own rest frame, we have:

$$v_{shk\rightarrow} = v_{x1} + c_{s1}\left[\frac{\left(\Gamma - 1\right)}{2\Gamma} + \frac{\left(\Gamma + 1\right)}{2\Gamma}\frac{P_2}{P_1}\right]$$

; Notice $v_{x2} \neq v_{shk\rightarrow}$

For ***left-going shocks*** we similarly have:

$$v_{x2} = v_{x1} - \left(P_2 - P_1\right)\sqrt{\frac{2\,V_1}{\left(\Gamma - 1\right)P_1 + \left(\Gamma + 1\right)P_2}}$$

To see why this shock is left-going, set $v_{x1} = 0$ to get $v_{x2} < 0$ . The shock velocity is:

$$v_{shk\leftarrow} = v_{x1} - c_{s1}\left[\frac{\left(\Gamma - 1\right)}{2\Gamma} + \frac{\left(\Gamma + 1\right)}{2\Gamma}\frac{P_2}{P_1}\right]$$

Focusing on right-going shocks we can plot out $v_{x2}$ for increasing values $P_2$ and any given pre-shock state ( $\rho_1$, $P_1$, $v_{x1}$) . The ***shock Hugoniot*** is shown below as the *solid line*. The analytic extension of the Hugoniot to include "*rarefaction shocks*" is shown via a *dashed line* and we will see this to be useful later on. A similar plot is shown for left-going shocks.

We see that progressively stronger right-going shocks produce increasing values of $v_{x2} - v_{x1}$. Progressively stronger left-going shocks produce decreasing values of $v_{x2} - v_{x1}$.

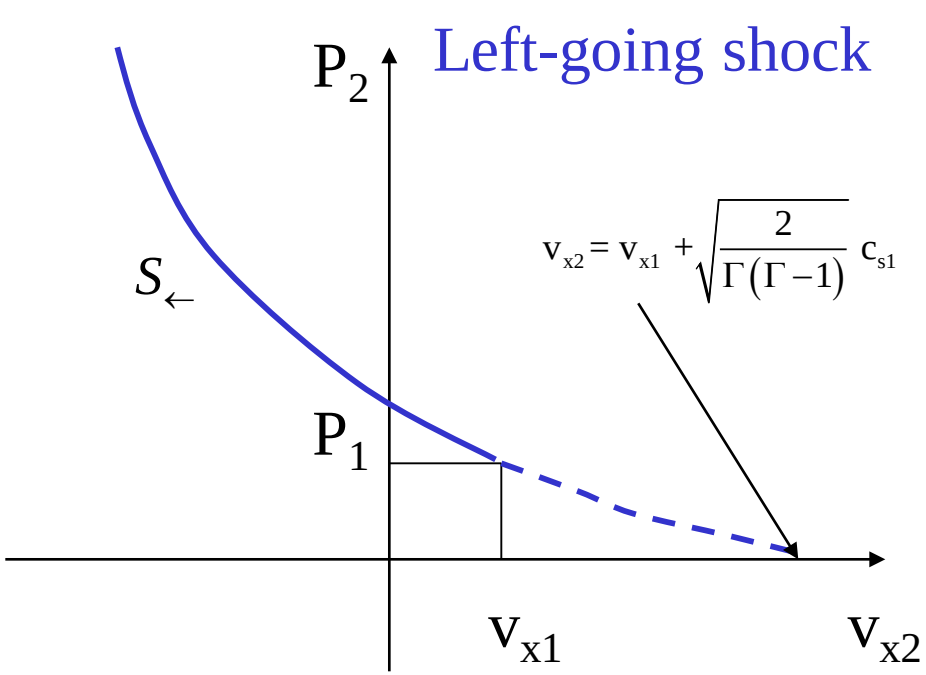


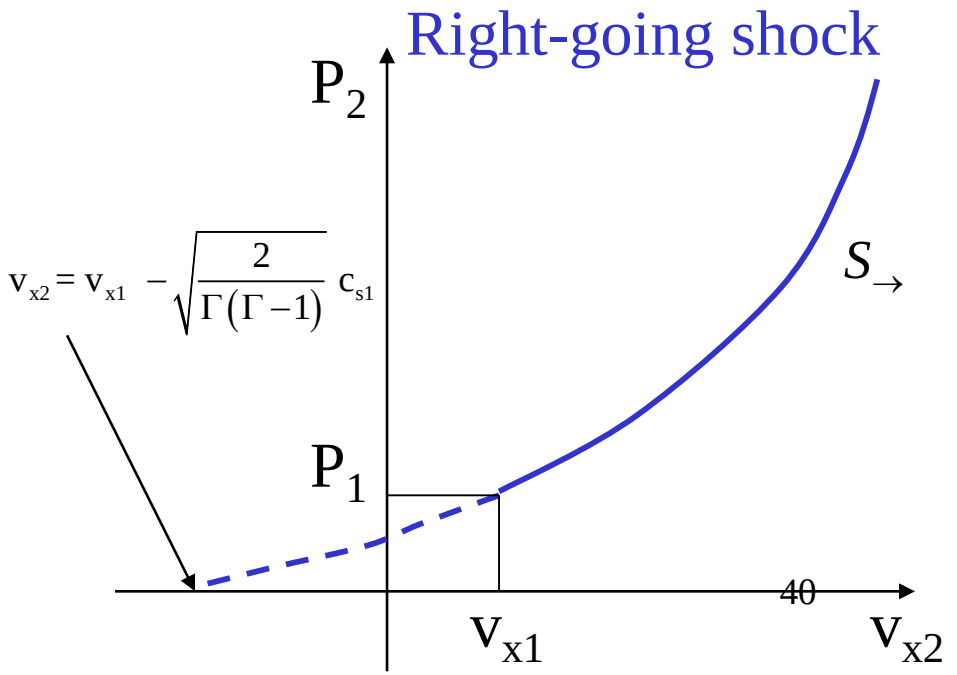

For a right-going shock, notice the following:

**a)** $v_{x2} - v_{x1} \rightarrow \infty$ as $P_2 \rightarrow \infty$ .

**b)** $\dfrac{\partial\left(v_{x2} - v_{x1}\right)}{\partial P_2} \rightarrow 0$ as $P_2 \rightarrow \infty$ ; i.e. in words, the velocity increase does not keep up with the pressure increase.

**c)** $P = 0$ at $v_{x2} - v_{x1} = -\sqrt{\dfrac{2}{\Gamma\left(\Gamma - 1\right)}}\, c_{s1}$ ; i.e. in words, there is a certain $-$ve velocity difference past which the pressure becomes zero in a rarefaction shock. In other words, the flow suffers a cavitation! We will see that a similar trend exists in real rarefaction fans. The only difference is that the rarefaction fan permits a larger range of $-$ve velocity difference before the cavitation sets in!

In a numerical code, an actual rarefaction fan opens up in a self-similar fashion as we have seen before. Once a rarefaction fan has opened up, the jump in flow variables from one zone to the next is rather small within the rarefaction fan. Consequently, for the sake of computational simplicity, it becomes acceptable to *replace actual rarefaction fans by (unphysical) rarefaction shocks. We do provide an* ***entropy fix*** *though*.

While unphysical, the dashed lines in the above plots nevertheless provide a reasonably good description of what happens in the total variation of flow variables across a rarefaction fan. We will elaborate on this point later.

Rarefaction shocks will, therefore, see use in place of rarefaction fans when constructing approximate Riemann solvers for astrophysical flow codes.

We will, however, not forget the central property of *rarefaction fans* that they *open up* in an entropy-preserving manner, while rarefaction shocks decrease the entropy in the post-shock region.

Thus while rarefaction shocks are often used in place of rarefaction fans during the iterative solution of the Riemann problem, we do need to go back post-facto and enforce an *entropy condition, i.e. an* ***entropy fix***, in the approximate Riemann solver.

# 5.3) Rarefaction Fans

We now focus on one dimensional continuous solutions that are isentropic. I.e., the entropy of a parcel of fluid does not change as the fluid moves around. ➔ no shocks develop.

While we specialize the equations in this section for ideal gases, we will also provide some general expressions for gases with real EOS.

For isentropic flow we have:

$$P = P_1 \left(\frac{\rho}{\rho_1}\right)^{\Gamma} \text{ which gives : } c_s = c_{s1}\left(\frac{\rho}{\rho_1}\right)^{\frac{\Gamma-1}{2}} ;\ \rho = \rho_1\left(\frac{c_s}{c_{s1}}\right)^{\frac{2}{\Gamma-1}} ;\ P = P_1\left(\frac{c_s}{c_{s1}}\right)^{\frac{2\Gamma}{\Gamma-1}}$$

Using the isentropic condition allows us to drop the entropy equation $S_t + \mathbf{v}\bullet\nabla S=0$. This is equivalent to dropping the thermal energy or total energy equations from the mix. The continuity and x-momentum equations then become:

$$\frac{1}{\rho}\left(\frac{\partial \rho}{\partial t} + v_x\frac{\partial \rho}{\partial x}\right) + \frac{\partial v_x}{\partial x} = 0 \ ;\ \left(\frac{\partial v_x}{\partial t} + v_x\frac{\partial v_x}{\partial x}\right) = -\frac{1}{\rho}\frac{\partial P}{\partial x}$$

Incorporating the isentropic relation $\frac{d\rho}{\rho} = \frac{2}{\Gamma - 1}\frac{dc_s}{c_s}$ we get:

$$\frac{\partial}{\partial t}\left(\frac{2}{\Gamma-1}c_s\right) + v_x \frac{\partial}{\partial x}\left(\frac{2}{\Gamma-1}c_s\right) + c_s \frac{\partial v_x}{\partial x} = 0 \; ; \; \frac{\partial v_x}{\partial t} + v_x \frac{\partial v_x}{\partial x} + c_s \frac{\partial}{\partial x}\left(\frac{2}{\Gamma-1}c_s\right) = 0$$

Adding and subtracting the above two equations gives:

$$\left[\frac{\partial}{\partial t} + (v_x + c_s)\frac{\partial}{\partial x}\right]\left(v_x + \frac{2}{\Gamma-1}c_s\right) = 0 \; ; \left[\frac{\partial}{\partial t} + (v_x - c_s)\frac{\partial}{\partial x}\right]\left(v_x - \frac{2}{\Gamma-1}c_s\right) = 0$$

These are the characteristic equations derived by Riemann. They tell us that :

$R \equiv v_x + \frac{2}{\Gamma-1}c_s$ remains constant along $\frac{dx}{dt} = v_x + c_s$ i.e. the $C_+$ characteristic.

$S \equiv v_x - \frac{2}{\Gamma-1}c_s$ remains constant along $\frac{dx}{dt} = v_x - c_s$ i.e. the $C_-$ characteristic.

R and S are known as the ***Riemann Invariants***.

$$P = P_1 \left( \frac{\rho}{\rho_1} \right)^{\Gamma} \; ; \; \rho = \rho_1 \left( \frac{c_s}{c_{s1}} \right)^{\frac{2}{\Gamma - 1}}$$

$$\frac{1}{\rho}\left( \frac{\partial \rho}{\partial t} + v_x \frac{\partial \rho}{\partial x} \right) + \frac{\partial v_x}{\partial x} = 0 \quad ; \quad \left( \frac{\partial v_x}{\partial t} + v_x \frac{\partial v_x}{\partial x} \right) = - \frac{1}{\rho} \frac{\partial P}{\partial x}$$

$$\left[ \frac{\partial}{\partial t} + \left( v_x + c_s \right) \frac{\partial}{\partial x} \right] \left( v_x + \frac{2}{\Gamma - 1} c_s \right) = 0 \; ; \left[ \frac{\partial}{\partial t} + \left( v_x - c_s \right) \frac{\partial}{\partial x} \right] \left( v_x - \frac{2}{\Gamma - 1} c_s \right) = 0$$

For a general EOS we have :

$$R \equiv v_x + l(\rho) \quad \text{and} \quad S \equiv v_x - l(\rho) \quad \text{where} \quad l(\rho) = \int_{\rho_1}^{\rho} \frac{c_s \, d\rho}{\rho} = \int_{P_1}^{P} \frac{dP}{\rho \, c_s}$$

R and S are the images of the characteristics $C_+$ and $C_-$ in the two-dimensional solution space ( $v_x$, $c_s$) .

For small fluctuations, it is easy to see that the above equations tell us how the fluctuations move. The eigenvectors give us similar information in the limit of small fluctuations. We see that the fluctuations move along the *characteristic curves* $C_+$ and $C_-$ .

But the above equations also go further. They tell us that the propagation of ***finite amplitude*** *isentropic fluctuations* can also be tracked as long as we track them along characteristics. This process can be continued as long as the characteristics of a given family do not intersect, i.e. as long as shocks don't form.

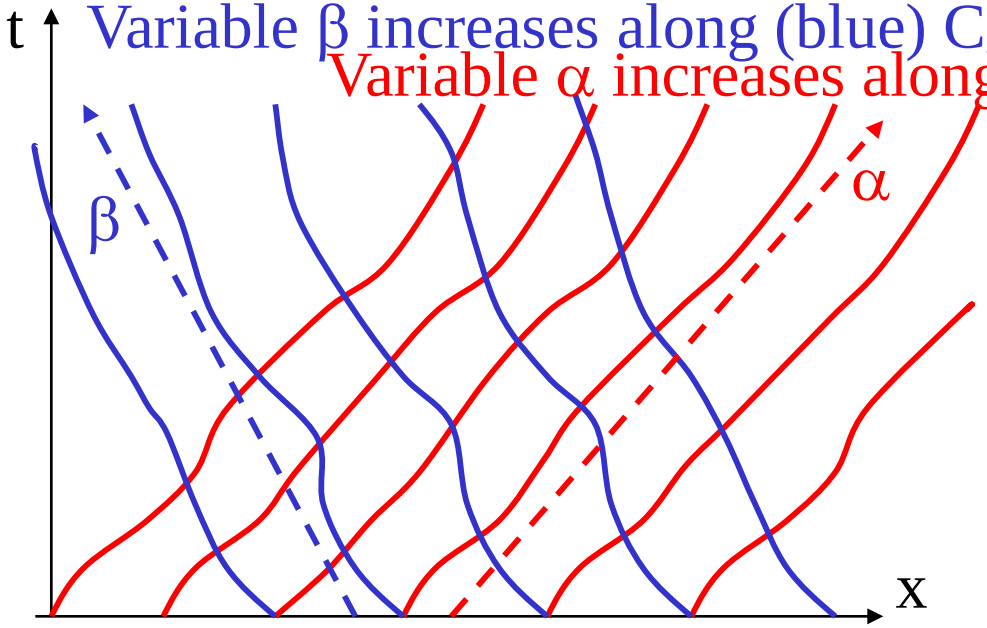


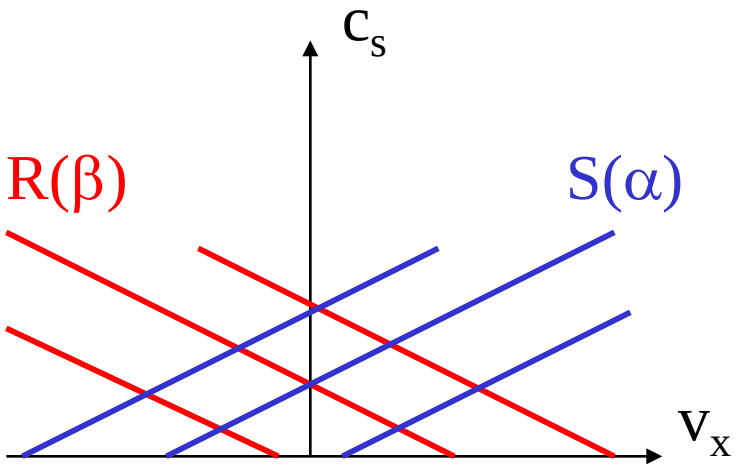


Consider the variables $\alpha$ and $\beta$ which increase in the time-like directions along the $C_+$ and $C_-$ characteristics respectively as shown in the figure. As long as characteristics of either family do not intersect with themselves, the two dimensional characteristic coordinate system formed by $(\alpha,\beta)$ provides an unusually easy coordinate system in which to read off the solution. In practice, the problem is implicit but say for simplicity that someone constructed an $(\alpha,\beta)$ coordinate system and even gave us $v_x(x)$ and $c_s(x)$. Then we can find the solution at any $(x,t)$ by reading off the corresponding $(\alpha,\beta)$ from the left fig. Then read off $R(\beta)$ and $S(\alpha)$ from the figure to the right. Then use $R(\beta)$ and $S(\alpha)$ to find $v_x(x,t)$ and $c_s(x,t)$.

In practice, constructing a characteristic coordinate system like the one shown in the above figure is never that simple. Question: Why? There are, however, simple flows for which explicit solution can be given.

These simple flows take the form of compression waves and *rarefaction fans*. Out of these, we are only interested in the latter but some of the development in this section is general enough to include the former.

These are ***simple waves*** for which either R or S is held constant all over space and time. This is tantamount to saying that the entire solution lies on only one of the straight lines in the ($v_x$, $c_s$) plane in the figure to the right above. As a result, v is always specified in terms of $c_s$ or vice versa.

A rarefaction fan usually forms next to a constant state of the flow. As a result, one of the families of characteristics finds its footpoint *starting from the constant state of the flow*. Consequently, that entire family corresponds to one and only *one single value of the corresponding Riemann invariant*.

A practical, mechanical example of a rarefaction fan occurs when a piston that is initially at rest in a tube of stationary gas is suddenly pulled out of the tube at a constant velocity.

The schematic and a space-time diagram of the characteristics is shown for the case where the piston is pulled to the left. Say the piston is initially at the origin.

Notice that all the left-going characteristics C_ must originate from the constant initial state in the gas and, therefore, must have the same value of the Riemann invariant $S_1 = -2\, c_{s1} / (\Gamma - 1)$. Here $c_{s1}$ is the sound speed in the initially static gas.

The fluid immediately abutting the piston must move with the piston's speed. Because we know rarefaction fans to be self-similar solutions, they can only depend on the ratio (x/t) .

Because $S_1$ is a constant along all $C_-$ , the only (isentropic) variation can be along the $C_+$ characteristics. To form a self-similar solution the $C_+$ characteristics, which are the only characteristics in this problem that can have non-trivial information propagating along them, must be straight lines in x-t space. Note though that ρ and $v_x$ may not have linear variation in x.

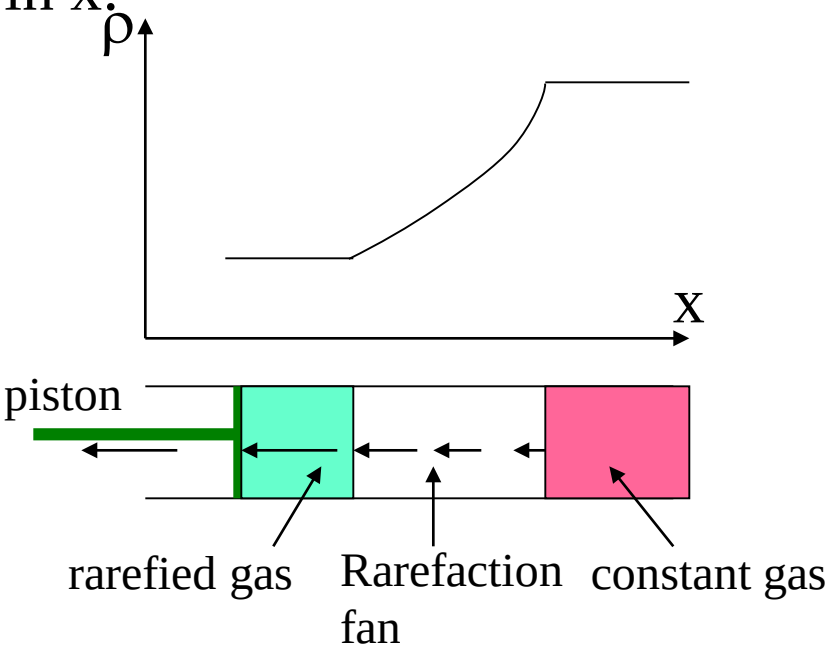


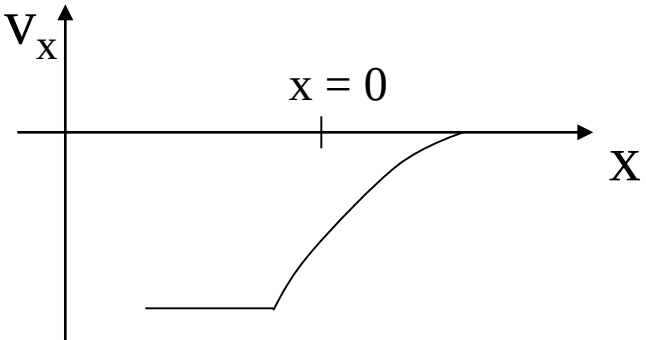


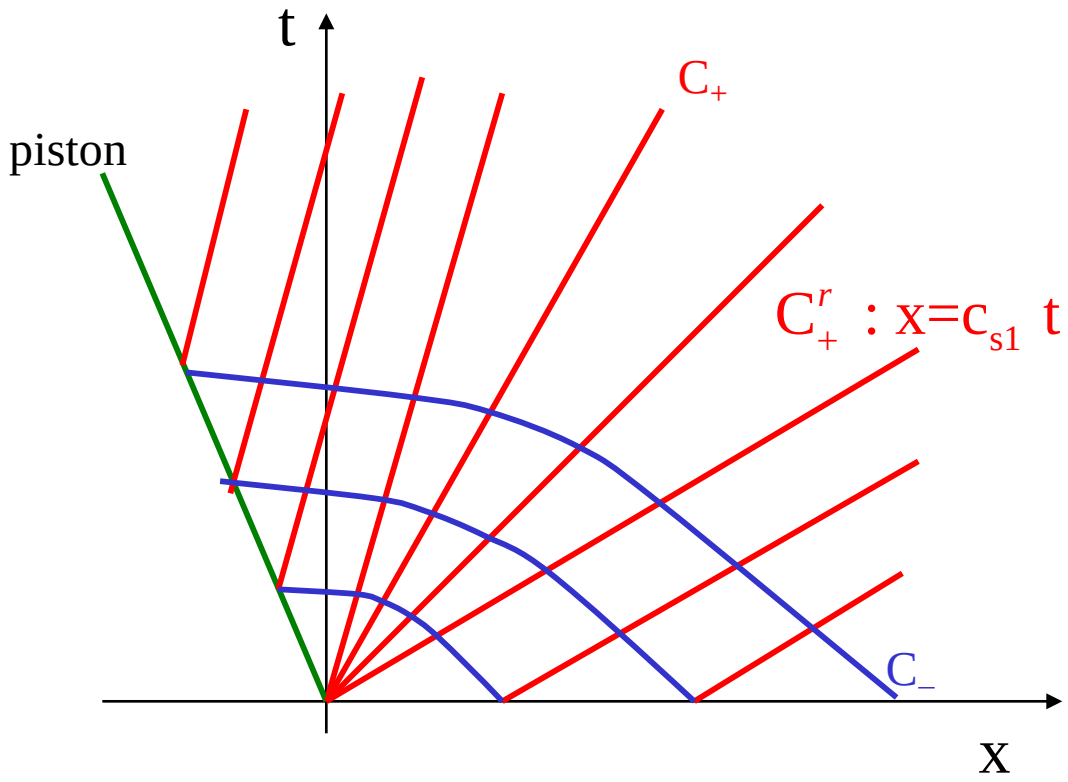

Notice that indeed at t=0 the solution has a discontinuity at x=0 .

Over time, a wave with locus $x = c_{s1}\, t$ moves into the gas to the right. i.e. over time, more and more parcels of gas flow into the rarefaction fan from its right. We, therefore, call it a right-going rarefaction fan.

This location of the right boundary of the rarefaction fan coincides with the first $C_+$ characteristic that varies with x/t. In other words, this characteristic, which is shown as the line $C_+^r$ in the above plot, is the right-most characteristic in the right-going rarefaction fan.

The left boundary of the rarefaction fan will correspond to a fluid state whose x-velocity matches that of the piston.

In the two next sub-sections we will study right- and left-going rarefaction fans, deriving expressions that are of general computational use. The derivation of the expressions for right-going fans will be given in full while the results for the left-going rarefaction fans will be stated without further detail since they closely parallel the previous results.

# 5.3.1) Right-going Rarefaction Fan

We have seen that for right-going simple waves we have a constant state to the right (applies to compression or rarefaction waves).

The Riemann invariant $S \equiv v_x - 2\,c_s/(\Gamma-1)$ remains constant.

Let us say that we have a constant state to the right of this wave and denote it by a subscript "1". Thus the state to the right is given by $(\rho_1, v_{x1}, v_{y1}, v_{z1}, P_1)$ with $c_{s1} = \sqrt{\Gamma\, P_1 / \rho_1}$ .

We can then assert : $v_x - \frac{2}{\Gamma-1} c_s = v_{x1} - \frac{2}{\Gamma-1} c_{s1}$ to get:

$$c_s = c_{s1} + \frac{(\Gamma-1)}{2}\left(v_x - v_{x1}\right)$$

$$\rho = \rho_1 \left(\frac{c_s}{c_{s1}}\right)^{\frac{2}{(\Gamma-1)}} = \rho_1 \left[1 + \frac{(\Gamma-1)}{2}\,\frac{\left(v_x - v_{x1}\right)}{c_{s1}}\right]^{\frac{2}{(\Gamma-1)}}$$

$$P = P_1 \left(\frac{c_s}{c_{s1}}\right)^{\frac{2\,\Gamma}{(\Gamma-1)}} = P_1 \left[1 + \frac{(\Gamma-1)}{2}\,\frac{\left(v_x - v_{x1}\right)}{c_{s1}}\right]^{\frac{2\,\Gamma}{(\Gamma-1)}}$$

$$S \equiv v_x - \frac{2}{\Gamma - 1} c_s = v_{x1} - \frac{2}{\Gamma - 1} c_{s1} \; ; \; \rho = \rho_1 \left( \frac{c_s}{c_{s1}} \right)^{\frac{2}{(\Gamma - 1)}} \; ; \; P = P_1 \left( \frac{c_s}{c_{s1}} \right)^{\frac{2\Gamma}{(\Gamma - 1)}}$$

$$c_s = c_{s1} + \frac{(\Gamma - 1)}{2} (v_x - v_{x1}) \; ; \; \rho = \rho_1 \left[ 1 + \frac{(\Gamma - 1)}{2} \frac{(v_x - v_{x1})}{c_{s1}} \right]^{\frac{2}{(\Gamma - 1)}}$$

$$P = P_1 \left[ 1 + \frac{(\Gamma - 1)}{2} \frac{(v_x - v_{x1})}{c_{s1}} \right]^{\frac{2\Gamma}{(\Gamma - 1)}} \Rightarrow \frac{(v_x - v_{x1})}{c_{s1}} \text{ measures strength of rarefaction}$$

The above three expressions are generally true for any right-going simple wave in a polytropic gas. We now specialize them for $C_+$ , i.e. right-going rarefaction fans that are initially centered at x=0. Such waves have the further special property that they obey a similarity solution that depends only on x/t. Furthermore, the $C_+$ characteristics carry that similarity information. This gives us:

$$\frac{x}{t} = v_x + c_s = v_{x1} + c_{s1} + \frac{(\Gamma+1)}{2}\left(v_x - v_{x1}\right)$$

or

$$v_x - v_{x1} = -\frac{2}{(\Gamma+1)}\left[\left(v_{x1} + c_{s1}\right) - \left(\frac{x}{t}\right)\right]$$

$$\rho = \rho_1 \left\{1 - \frac{(\Gamma-1)}{(\Gamma+1)}\frac{1}{c_{s1}}\left[\left(v_{x1} + c_{s1}\right) - \left(\frac{x}{t}\right)\right]\right\}^{\frac{2}{(\Gamma-1)}}$$

$$P = P_1 \left\{1 - \frac{(\Gamma-1)}{(\Gamma+1)}\frac{1}{c_{s1}}\left[\left(v_{x1} + c_{s1}\right) - \left(\frac{x}{t}\right)\right]\right\}^{\frac{2\,\Gamma}{(\Gamma-1)}}$$

$$c_s = c_{s1} + \frac{(\Gamma - 1)}{2}\left(v_x - v_{x1}\right) \quad ; \quad P = P_1\left[1 + \frac{(\Gamma - 1)}{2}\,\frac{\left(v_x - v_{x1}\right)}{c_{s1}}\right]^{\frac{2\,\Gamma}{(\Gamma - 1)}}$$

$$\frac{x}{t} = v_x + c_s =$$

$$v_x - v_{x1} = -\,\frac{2}{(\Gamma + 1)}\left[\left(v_{x1} + c_{s1}\right) - \left(\frac{x}{t}\right)\right] \quad ; \quad P = P_1\left\{1 - \frac{(\Gamma - 1)}{(\Gamma + 1)}\,\frac{1}{c_{s1}}\left[\left(v_{x1} + c_{s1}\right) - \left(\frac{x}{t}\right)\right]\right\}^{\frac{2\,\Gamma}{(\Gamma - 1)}}$$

Notice that for a centered rarefaction fan the right-most $C_+$ characteristic that belongs to the fan is given by $x = \left(v_{x1} + c_{s1}\right) t$ . As one traverses the fan from right to left, $\left[\left(v_{x1} + c_{s1}\right) - \left(\frac{x}{t}\right)\right]$ increases. Consequently, $v_x$ decreases monotonically from $v_{x1}$ , P decreases monotonically from $P_1$ and $\rho$ decreases monotonically from $\rho_1$ as the right-going rarefaction fan is traversed from right to left.

If we denote the variables to the left of the right-going rarefaction fan by $(\rho_2 , v_{x2} , v_{y1} , v_{z1} , P_2)$ we see that $v_{x2} - v_{x1} < 0$ , $P_2 < P_1$ and $\rho_2 < \rho_1$ . These trends run exactly opposite to the trends observed for a right-going shock.

---

When solving the Riemann problem, special attention will have to be paid to those situations where an *open rarefaction fan* straddles a zone boundary. The above expressions are very useful when obtaining the resolved state at a moving (or stationary) zone boundary when a $C_+$ rarefaction fan straddles that boundary.

For example, we say that the $C_+$ rarefaction fan is open and straddles the zone boundary x=0 if $\lambda_1 = v_{x1} + c_{s1} > 0$ and $\lambda_2 = v_{x2} + c_{s2} < 0$.

As in the case of shocks, we find that the ratio $P_2/P_1$ is also a good measure of the strength of a rarefaction fan.

When obtaining a numerical solution of the Riemann problem, it helps to iterate the problem towards a converged solution using one judiciously chosen iteration variable. For shocks we see that the post-shock pressure $P_2$ is such a good variable. The previous point has shown that the pressure $P_2$ behind a rarefaction fan is a similarly good variable. We, therefore, obtain expressions for $v_{x2} - v_{x1}$ and $\rho_2$ in terms of the variables in front of the rarefaction fan and the ratio $P_2/P_1$ .

$$v_{x2} - v_{x1} = -\frac{2\,c_{s1}}{(\Gamma - 1)}\left[1 - \left(\frac{P_2}{P_1}\right)^{\frac{(\Gamma-1)}{2\Gamma}}\right] \quad ; \quad \rho_2 = \rho_1 \left(\frac{P_2}{P_1}\right)^{\frac{1}{\Gamma}}$$

$$v_x - v_{x1} = -\frac{2}{(\Gamma+1)}\left[(v_{x1}+c_{s1})-\left(\frac{x}{t}\right)\right] \;;\; P = P_1\left\{1 - \frac{(\Gamma-1)}{(\Gamma+1)}\frac{1}{c_{s1}}\left[(v_{x1}+c_{s1})-\left(\frac{x}{t}\right)\right]\right\}^{\frac{2\Gamma}{(\Gamma-1)}}$$

$$v_{x2} - v_{x1} = -\frac{2\,c_{s1}}{(\Gamma-1)}\left[1 - \left(\frac{P_2}{P_1}\right)^{\frac{(\Gamma-1)}{2\Gamma}}\right]$$

The above expression can be viewed as an *adiabat for right-going rarefactions* similar to the Hugoniot adiabat for right-going shocks. In fact, it proves most instructive to plot them out on the same plot assuming $1 < \Gamma < 2$ , which is the usual case.

Solid red curve shows right-going rarefaction, solid blue a right-going shock. The dashed curves of either color are analytic extensions.

Right-going shock v/s Right-going Rarefaction Fan

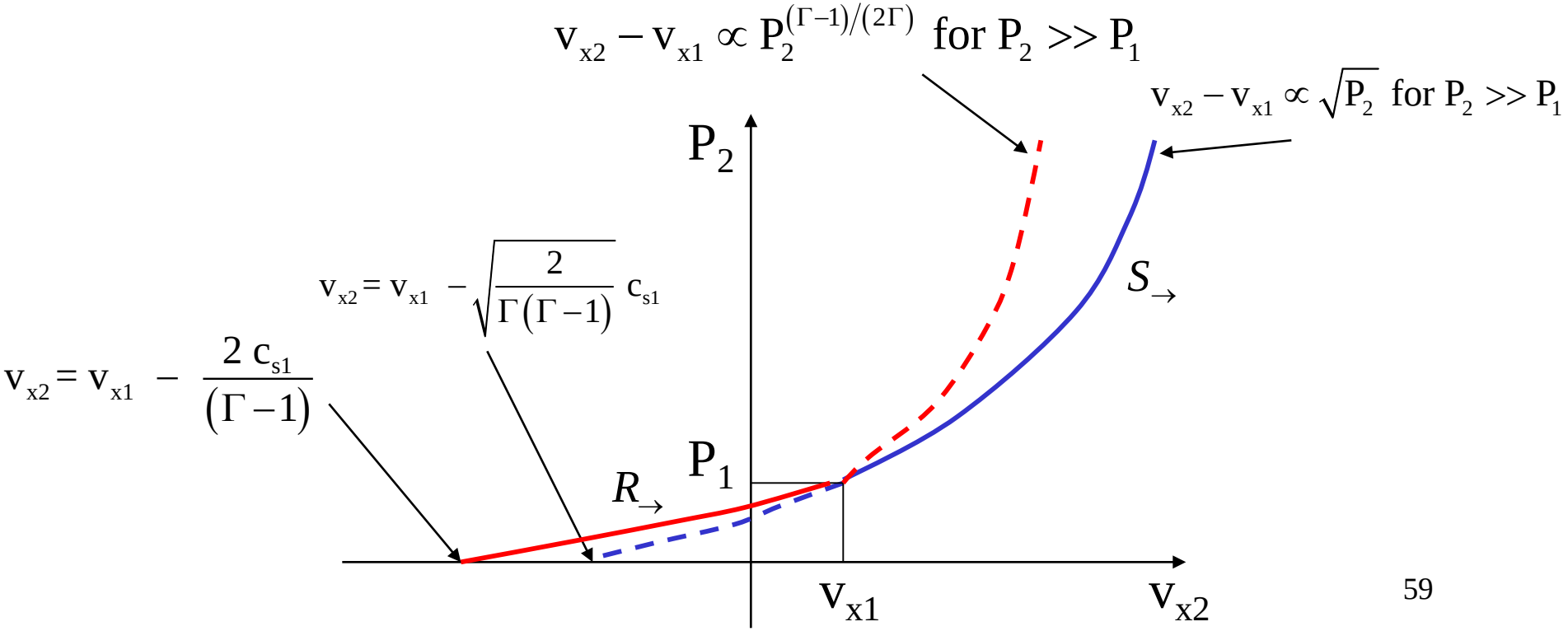

We see that for $P_2 \sim P_1$ *both adiabats have the same slope*. This is as expected. It means that for weak shocks or weak rarefactions it does not matter whether we use either adiabat.

We also notice that for $v_{x2} - v_{x1} < 0$, the *rarefaction fan permits a larger velocity difference before developing a cavitation* than a rarefaction shock. As a result, an exact Riemann solver, which uses rarefaction fans, will do a little better than an approximate Riemann solver that replaces rarefaction fans by rarefaction shocks.

In practice, the above gain is slight. We will see in the next chapter that there are other Riemann solvers that resist the formation of cavitations even better than the exact Riemann solver.

We also see that for $P_2 >> P_1$ , i.e. for strong shocks, the *rarefaction adiabat and the shock adiabat have very different asymptotic behaviors*. It is for this reason that efforts to replace shock adiabats by rarefaction adiabats even in the compressive part where $P_2 > P_1$ have not met with much success. (See Osher and Solomon's Riemann solver for example.)

# 6.3.b) Left-going Rarefaction Fan

We have seen that for left-going simple waves we have a constant state to the left (applies to compression or rarefaction waves).

The Riemann invariant $R \equiv v_x + 2\,c_s/(\Gamma-1)$ remains constant.

As before, we have a constant state to the left of this wave and we denote it by a subscript "1". Thus the state is given by $(\rho_1, v_{x1}, v_{y1}, v_{z1}, P_1)$

with $c_{s1}=\sqrt{\Gamma\, P_1/\rho_1}$ .

We can then assert : $v_x + \frac{2}{\Gamma-1}c_s = v_{x1} + \frac{2}{\Gamma-1}c_{s1}$ to get:

$$c_s = c_{s1} - \frac{(\Gamma-1)}{2}\left(v_x - v_{x1}\right)$$

$$\rho = \rho_1\left(\frac{c_s}{c_{s1}}\right)^{\frac{2}{(\Gamma-1)}} = \rho_1\left[1 - \frac{(\Gamma-1)}{2}\frac{\left(v_x - v_{x1}\right)}{c_{s1}}\right]^{\frac{2}{(\Gamma-1)}}$$

$$P = P_1\left(\frac{c_s}{c_{s1}}\right)^{\frac{2\,\Gamma}{(\Gamma-1)}} = P_1\left[1 - \frac{(\Gamma-1)}{2}\frac{\left(v_x - v_{x1}\right)}{c_{s1}}\right]^{\frac{2\,\Gamma}{(\Gamma-1)}}$$

The above expressions are generally true for any left-going simple wave in a polytropic gas. We now specialize them for C_ , i.e. left-going self-similar rarefaction fans that are initially centered at x=0. We get:

$$v_x - v_{x1} = \frac{2}{(\Gamma+1)}\left[\left(\frac{x}{t}\right) - (v_{x1} - c_{s1})\right]$$

$$\rho = \rho_1 \left\{1 - \frac{(\Gamma-1)}{(\Gamma+1)} \frac{1}{c_{s1}} \left[\left(\frac{x}{t}\right) - (v_{x1} - c_{s1})\right]\right\}^{\frac{2}{(\Gamma-1)}}$$

$$P = P_1 \left\{1 - \frac{(\Gamma-1)}{(\Gamma+1)} \frac{1}{c_{s1}} \left[\left(\frac{x}{t}\right) - (v_{x1} - c_{s1})\right]\right\}^{\frac{2\Gamma}{(\Gamma-1)}}$$

Notice that $\left(\frac{x}{t}\right) - (v_{x1} - c_{s1})$ is positive and monotonically increasing as one traverses a left-going rarefaction fan from left to right.

If we denote the variables to the right of the left-going rarefaction fan by $(\rho_2, v_{x2}, v_{y1}, v_{z1}, P_2)$ we see that $v_{x2} - v_{x1} > 0$, $P_2 < P_1$ and $\rho_2 < \rho_1$.

These trends run exactly opposite to the trends observed for a left-going shock.

---

We, now obtain expressions for $v_{x2} - v_{x1}$ and $\rho_2$ in terms of the variables in front of the rarefaction fan and the ratio $P_2/P_1$.

$$v_{x2} - v_{x1} = \frac{2\, c_{s1}}{(\Gamma - 1)}\left[1 - \left(\frac{P_2}{P_1}\right)^{\frac{(\Gamma-1)}{2\Gamma}}\right] \quad ; \quad \rho_2 = \rho_1 \left(\frac{P_2}{P_1}\right)^{\frac{1}{\Gamma}}$$

The above expression can be viewed as an adiabat for left-going rarefactions similar to the Hugoniot adiabat for left-going shocks. In fact, it proves most instructive to plot them out on the same plot assuming $1 < \Gamma < 2$, which is the usual case.

Solid red curve shows left-going rarefaction, solid blue a left-going shock. The dashed curves of either color are analytic extensions.

The figure shows that all the same anticipated trends in the limits $P_2 \sim P_1$ , $P_2 << P_1$ and $P_2 >> P_1$ are reproduced here even for the left-going waves. As a result, the following plot leads us to conclusions that are similar to the ones reached in the previous section.

## Left-going shock v/s left-going rarefaction

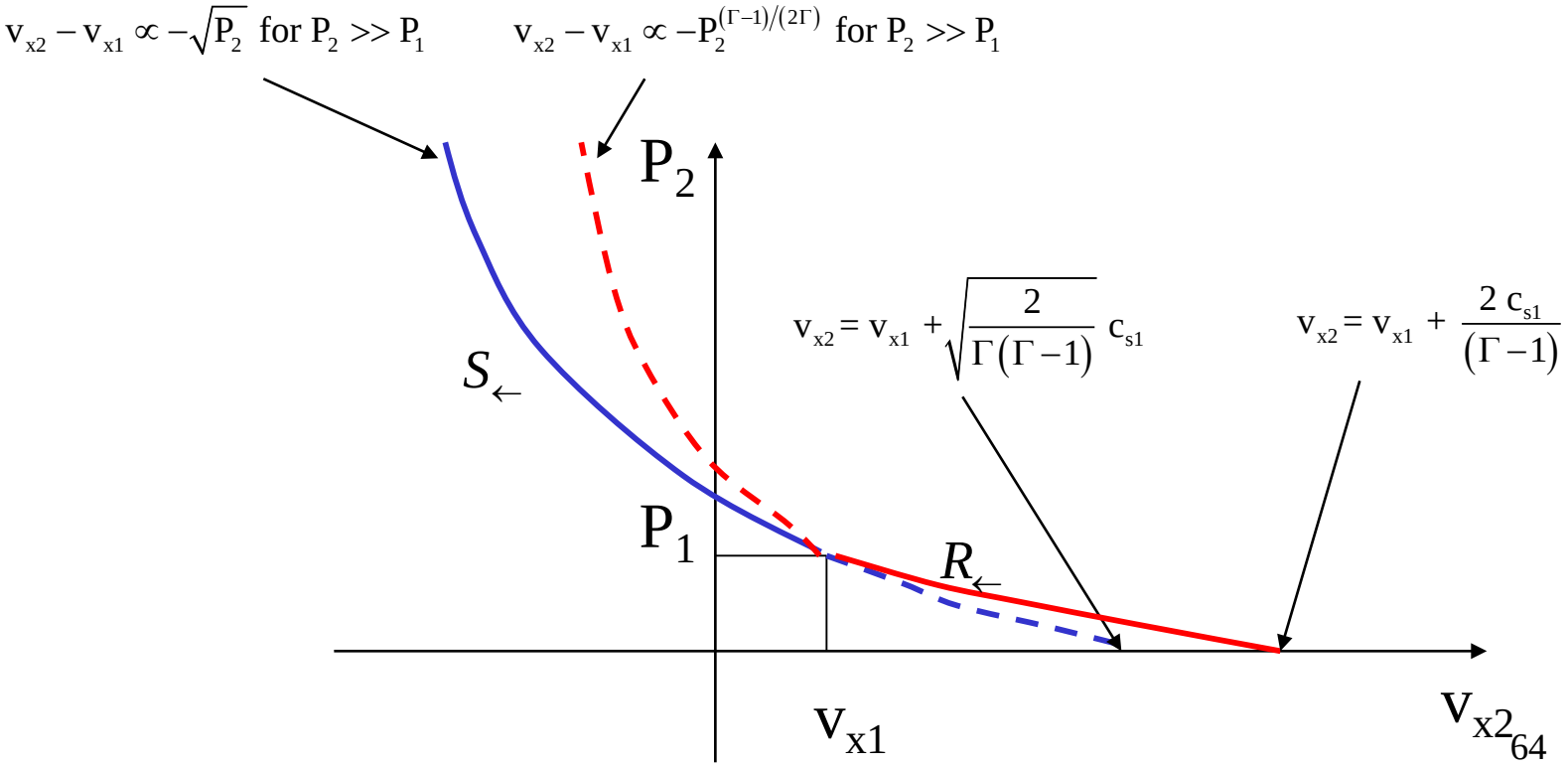

# 5.4) The Riemann Problem

## 5.4.1) Intuitive Introduction to the Riemann Problem

Riemann envisioned a situation where two initially uniform slabs of gas are brought into contact at the plane x=0 and then allowed to evolve self consistently in one dimension along the x-axis. Call the initial variables to the left ($\rho_{1L}$, $v_{x1L}$, $v_{y1L}$, $v_{z1L}$, $P_{1L}$) and call the corresponding initial flow variables to the right ($\rho_{1R}$, $v_{x1R}$, $v_{y1R}$, $v_{z1R}$, $P_{1R}$) . The Riemann problem describes the subsequent evolution of that flow.

Riemann's important realization what that the problem can only evolve as a *similarity solution* in the x-t space. The only self-similar fluid dynamical structures that we know of are shock waves, centered rarefaction fans and contact discontinuities.

In such flow structures the information (Riemann invariants) are constant along certain characteristic families and the only jump in variables occurs at shocks.

Assuming that the problem is well-defined, and assuming that cavitations do not form, Riemann asserted that there are only four possible outcomes of such a problem:

***i)*** *right- & left-going shocks*,
***ii)*** *right-going shock & left-going rarefaction fan*,
***iii)*** *left-going shock & right-going rarefaction fan*,
***iv)*** *right- & left-going rarefaction fans*.

In all such cases, a *contact discontinuity* between the two elementary flow structures preserves the original sanctity of the two slabs of fluid. Across the contact discontinuity we have a jump in entropy as well as a jump in transverse velocity.

If the two fluids in the two initial slabs have different properties, such as different polytropic indices or different composition, then that that difference is preserved across the contact discontinuity.

Given the information presented in the Introduction of this chapter it is evident that the Riemann problem plays a very important role in compressible flow calculations.

The case where $P_{1L} > P_{1R}$ , $\rho_{1L} > \rho_{1R}$ with all the initial velocities zeroed is particularly interesting because of its relevance to shock tubes. The problem corresponds to the figure that was presented schematically in the introduction. It is also rather simple to analyze. We do that next.

Since the pressure to the left is higher, it sends a right-going shock into the fluid to the right with a pressure P* that is intermediate between $P_{1L}$ and $P_{1R}$ . All the $C_+$ characteristics in the left fluid will have their footpoints in the constant flow to the left. Since $P^* < P_{1L}$ the only self-similar flow that can establish itself in the left fluid is a left-going rarefaction fan. The density in the post-shock gas that lies to the left of the right-going shock and the density in the gas that lies to the right of the left-going rarefaction fan will not match in general. As a result, a contact discontinuity develops with the same pressure P* and velocity $v_{x2}^*$ on both sides of it.

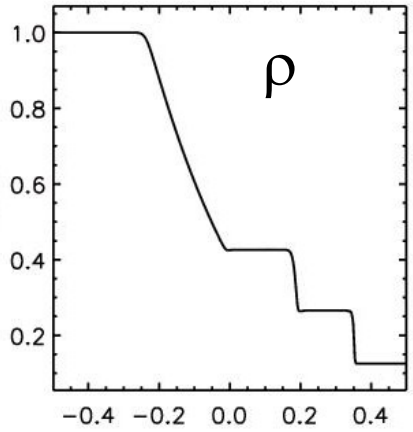


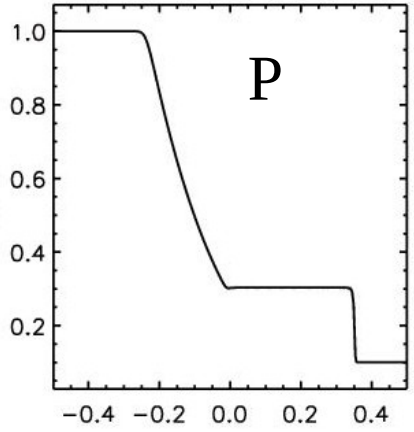


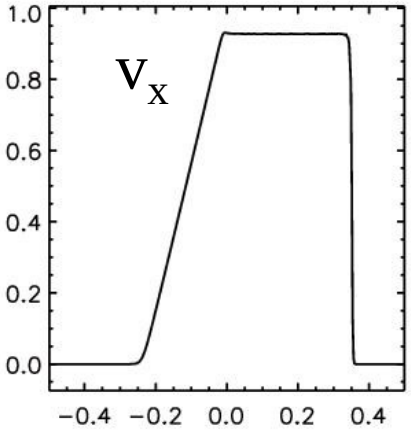


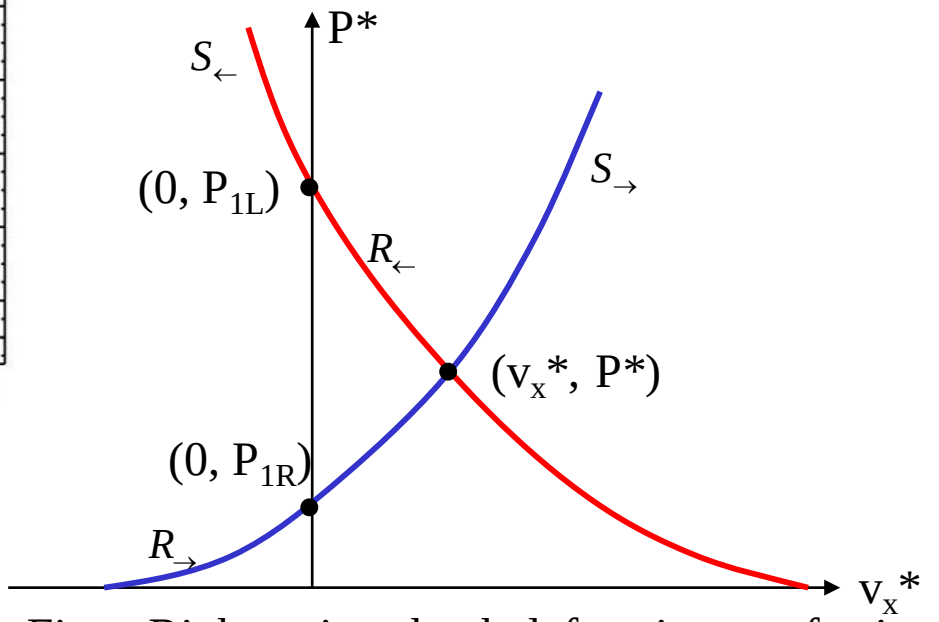


Fig. a Right-going shock, left-going rarefaction

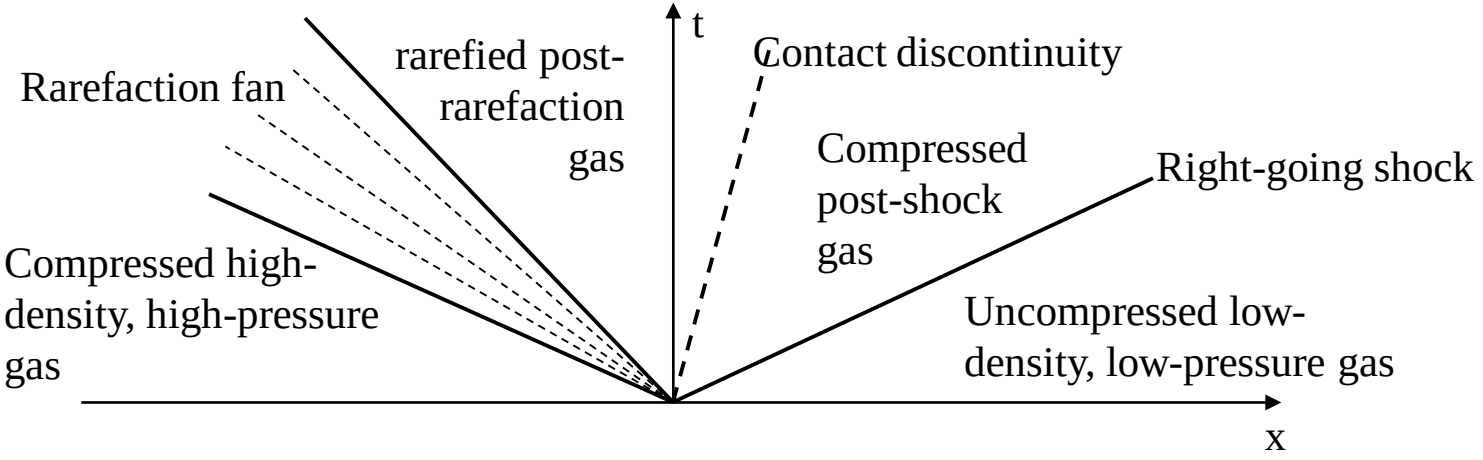

The next figure depicts the same situation intuitively. Focus on Fig. a which shows a slightly more general situation where the left and right velocities of the initial states do not have to be zero. The right state is shown by the point ($v_{x1R}$, $P_{1R}$) on the blue line and has lower pressure than the left state which is shown by the point ($v_{x1L}$, $P_{1L}$) on the red line. The blue curve in the plot is the locus of all right-going waves that can connect to the initial right state ($v_{x1R}$, $P_{1R}$) . As a result it increases to the right, similar to the situation depicted in the Fig. for right-going waves. We see that the right state can only have a right-going wave passing through it once the problem evolves. If the *intermediate state* is ($v_x$*, P*) then the right-going wave will be a shock if $P^* > P_{1R}$ and a rarefaction if $P^* < P_{1R}$ . The red line is the locus of all left-going waves that can connect to the initial left state ($v_{x1L}$, $P_{1L}$) . Notice that since the red curve represents a left-going wave, it decreases to the right, similar to the situation depicted in the Fig. for left-going waves. As a result, the red and blue curves are guaranteed to intersect. The location of the intermediate state ($v_x$*, P*) in Fig. a shows that the resolved Riemann problem has a right-going shock and a left-going discontinuity.

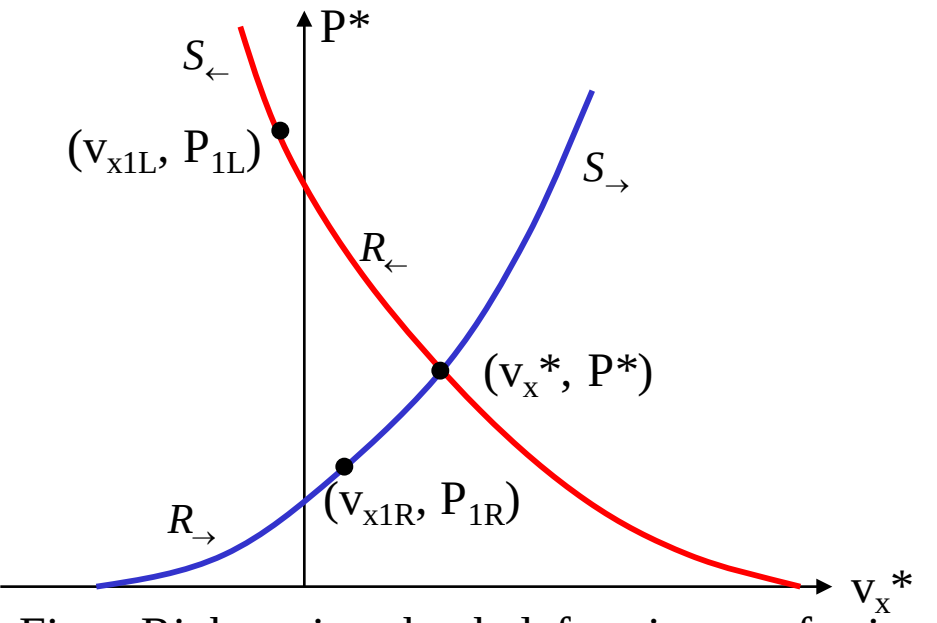


Fig. a Right-going shock, left-going rarefaction

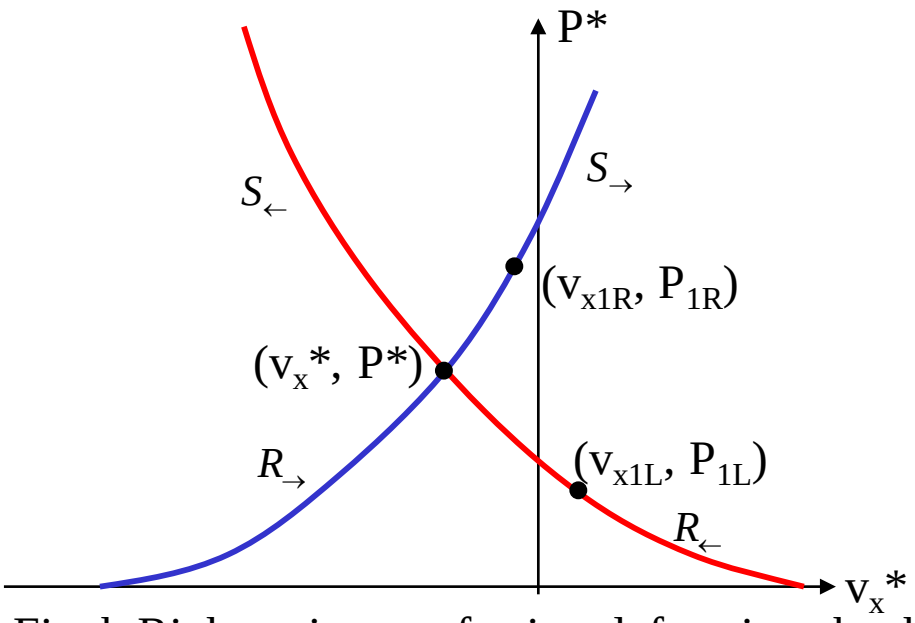


Fig. b Right-going rarefaction, left-going shock

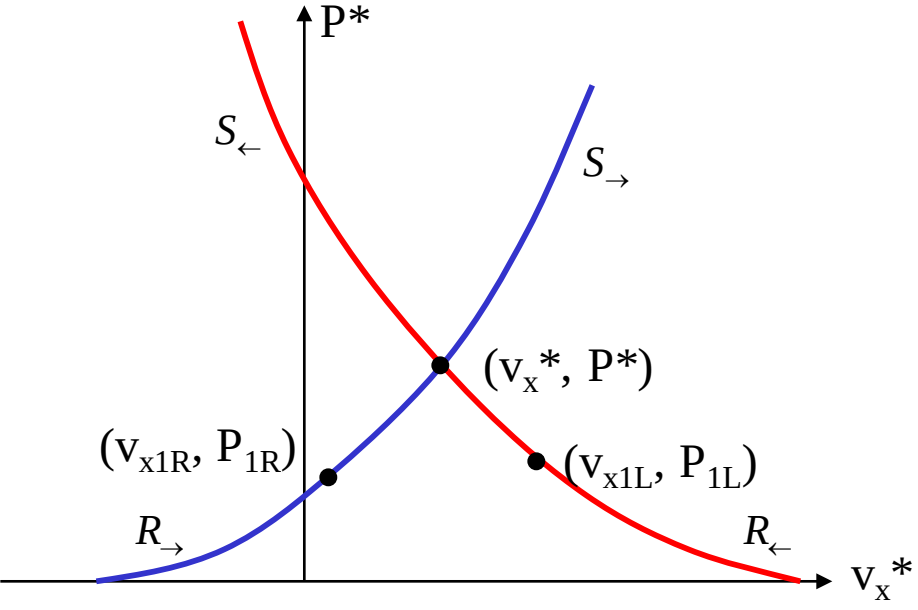


Fig. c Right-going shock, left-going shock

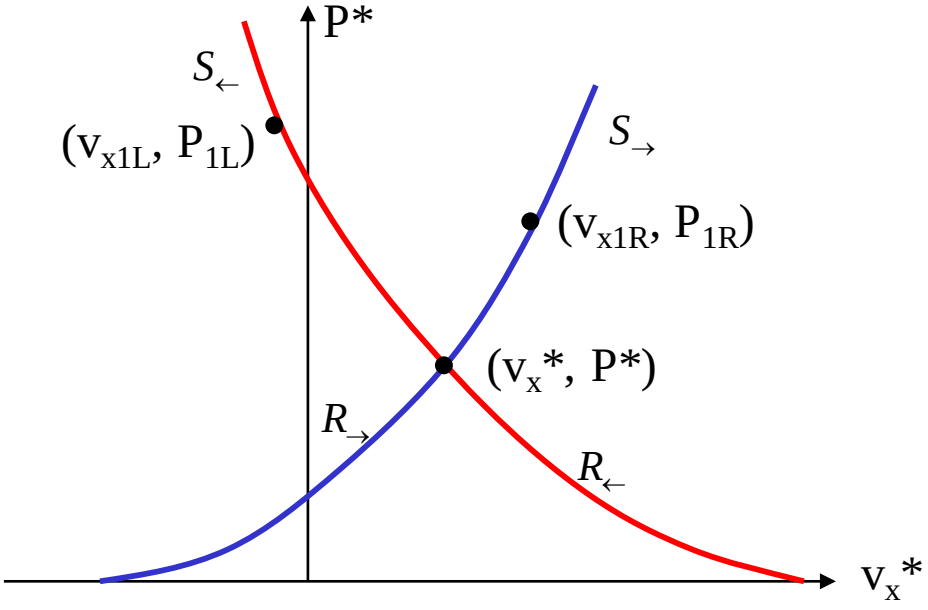


Fig. d Right-going rarefaction, left-going rarefactio

Question: Now that Fig. a has been analyzed for you, can you similarly analyze Figs. b, c and d ?

Question: The next two figures show you actual, computed solutions of the Riemann problem. Can you match the generic situations depicted in the previous plots to the specific Riemann problems shown on the next two pages?

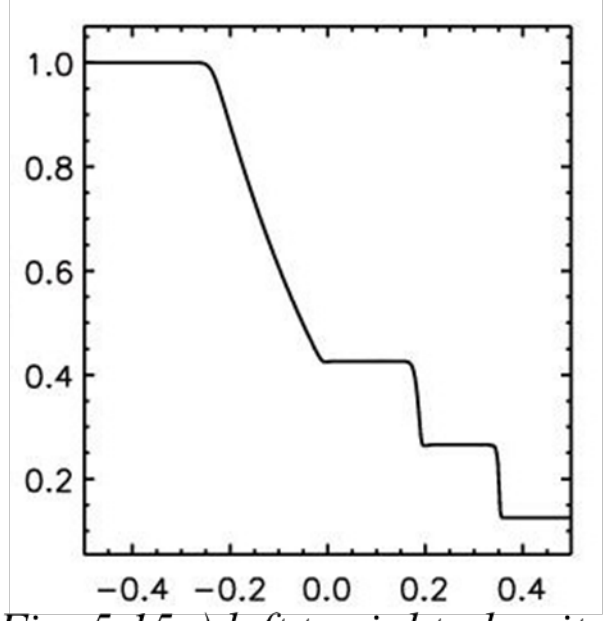

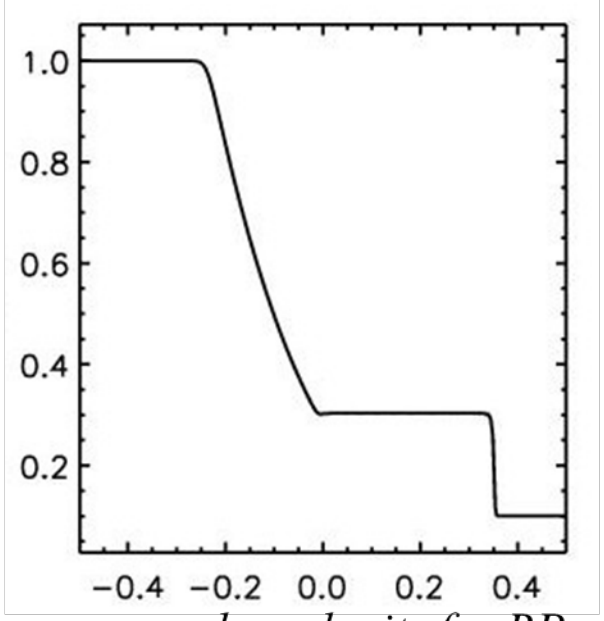

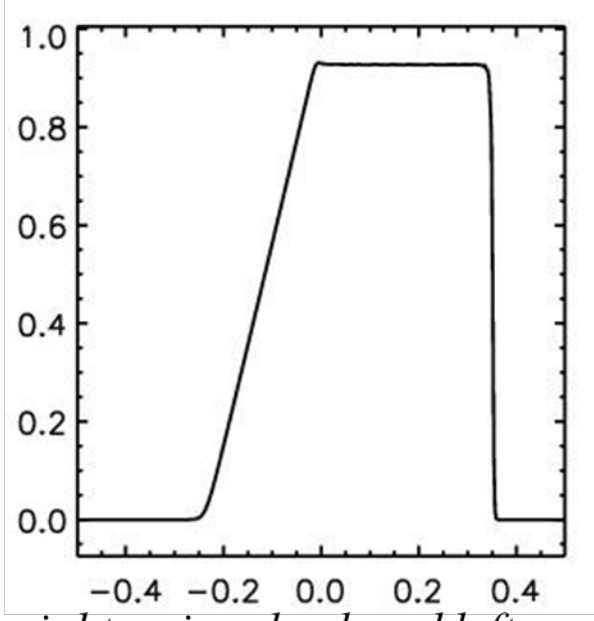


*Fig. 5.15a) left to right: density, pressure and x-velocity for RP with right-going shock and left-going rarefaction*

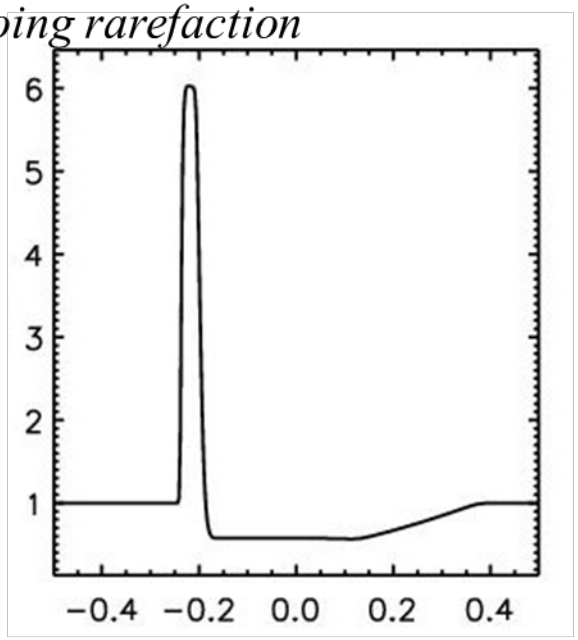

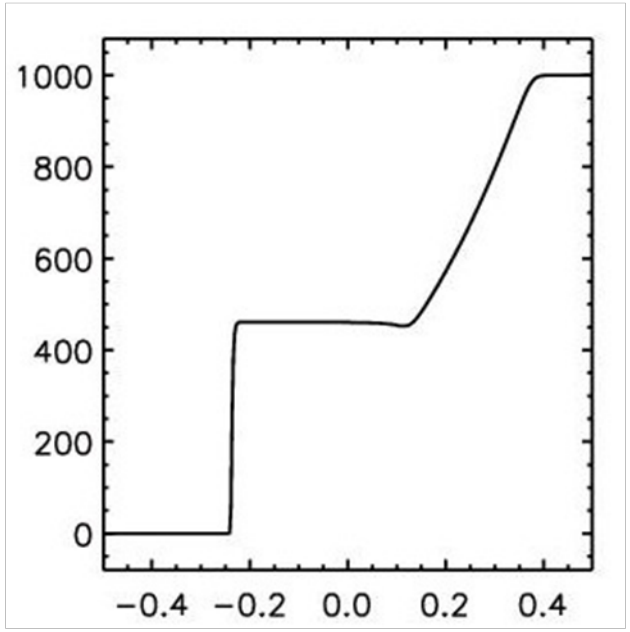

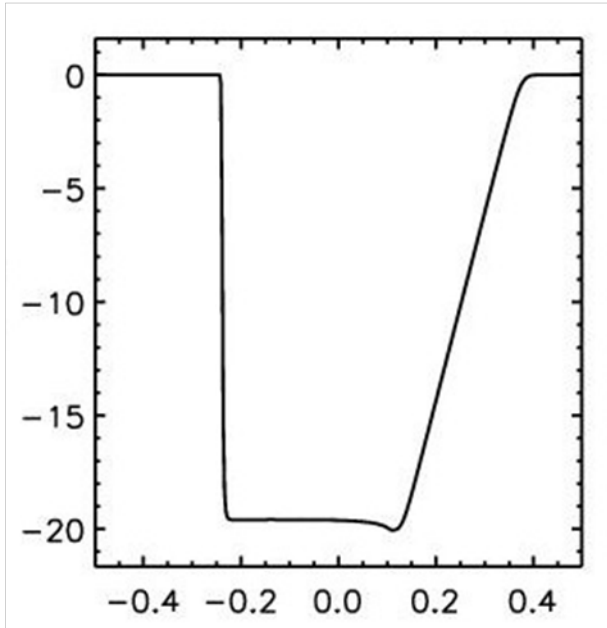


*Fig. 5.15b) left to right: density, pressure and x-velocity for RP with left-going shock and right-going rarefaction*

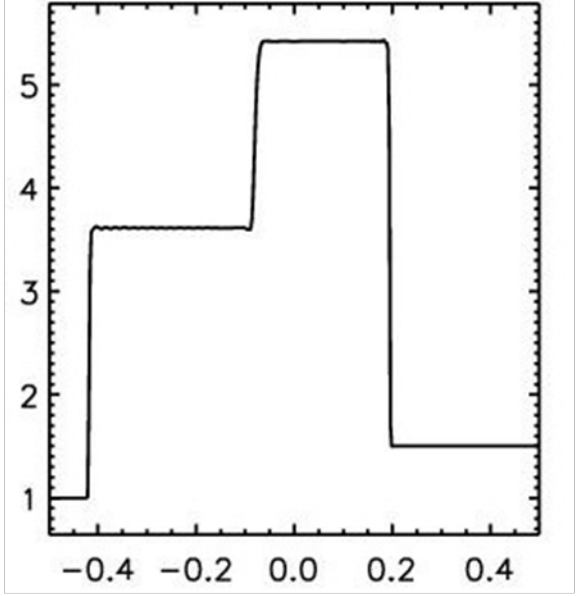

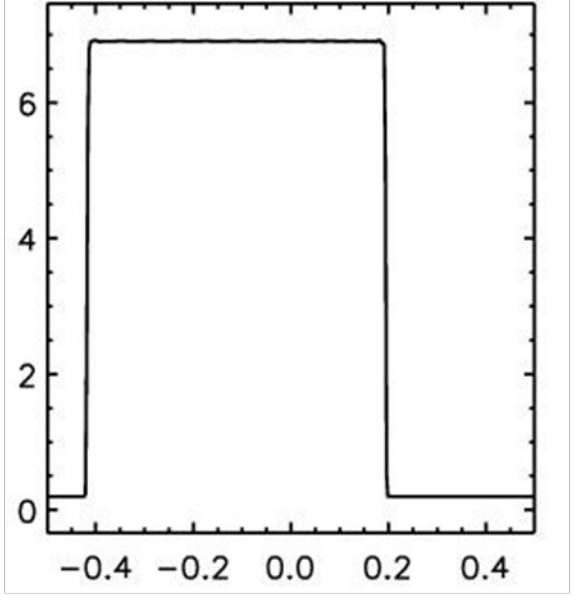

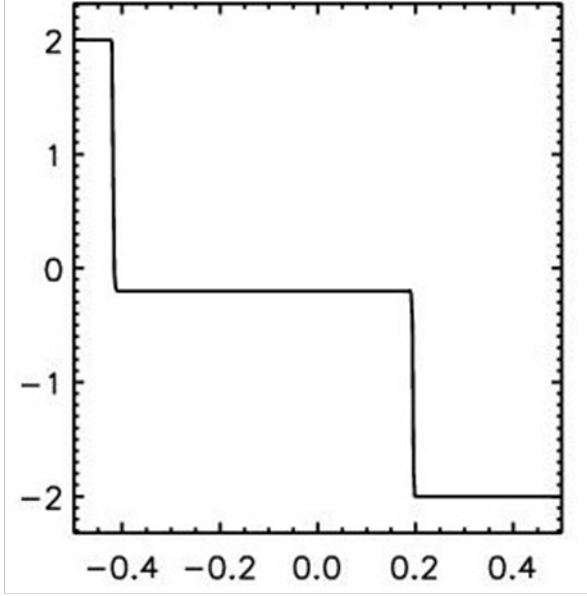


*Fig. 5.16a) left to right: density, pressure and x-velocity for RP with right- and left-going shocks*

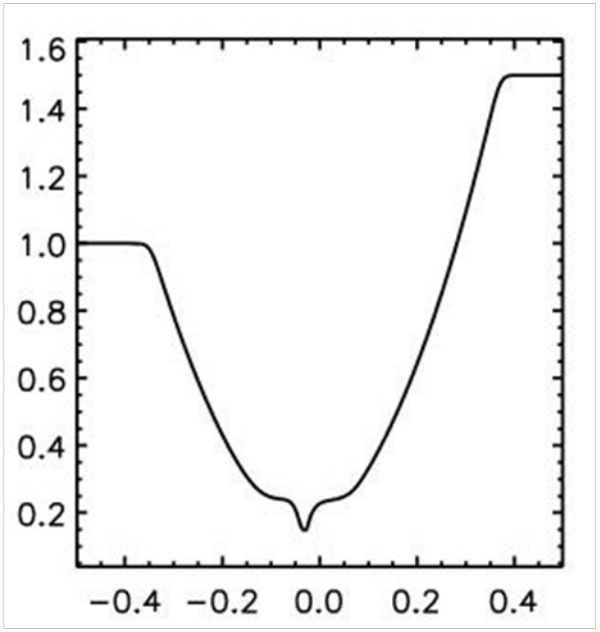

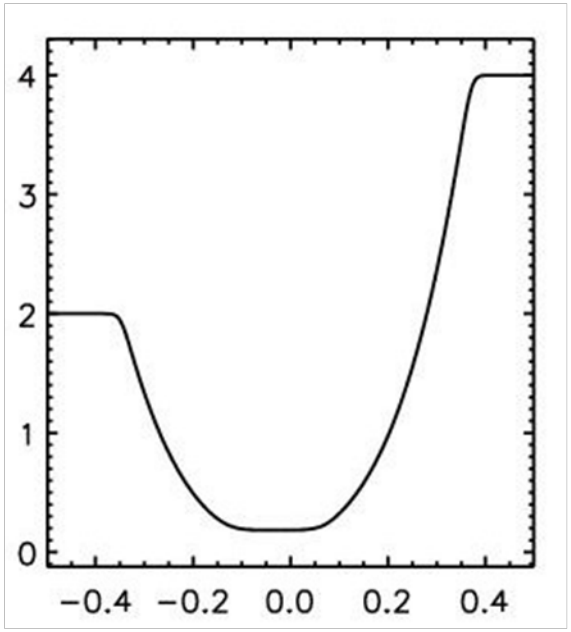

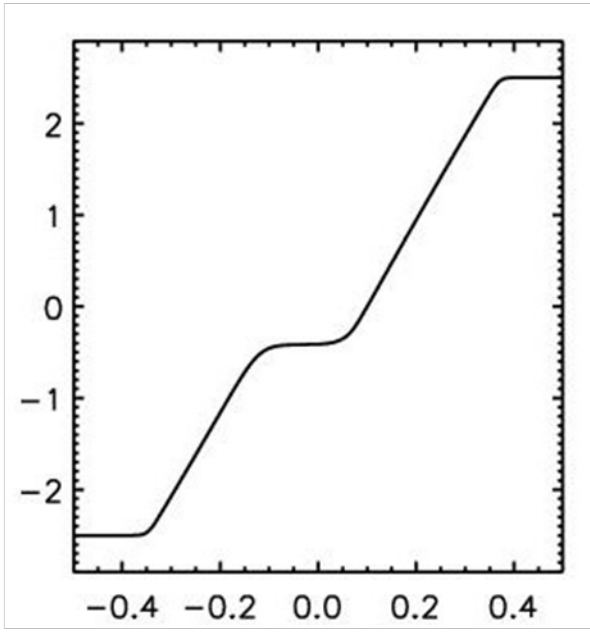


*Fig. 5.16b) left to right: density, pressure and x-velocity for RP with right- and left-going rarefaction fans*

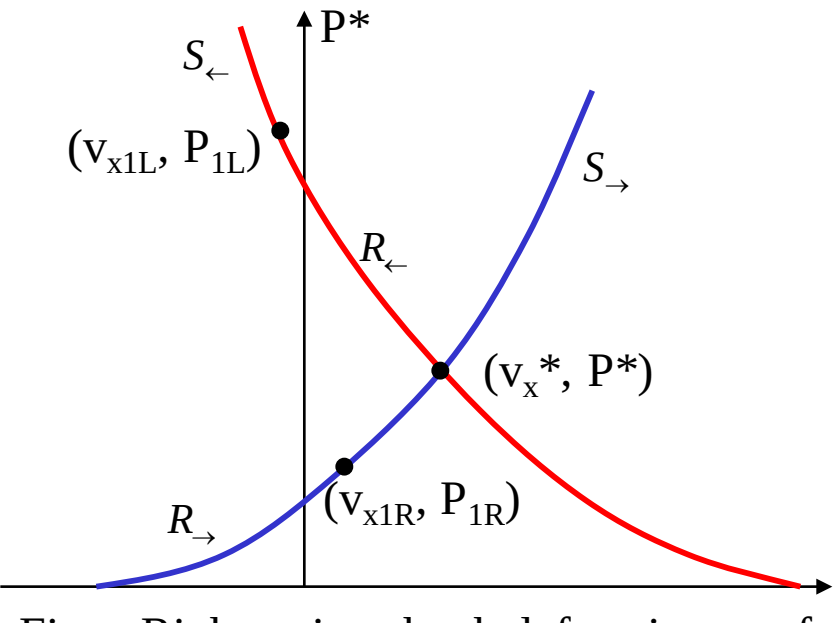


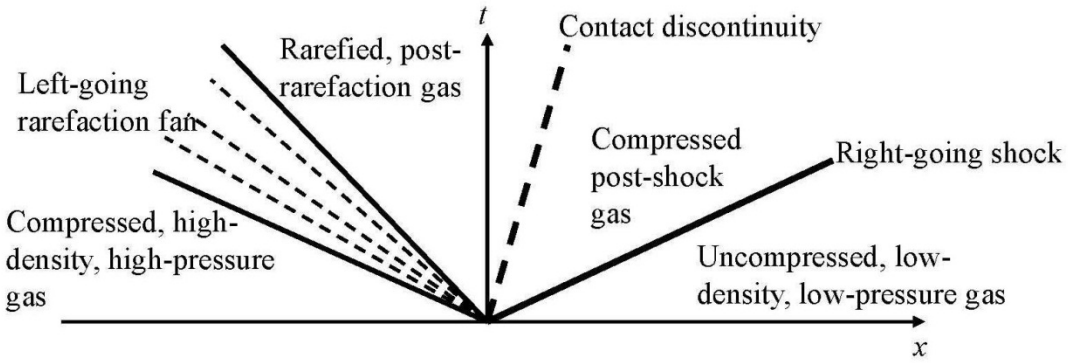


Fig. a Right-going shock, left-going rarefaction

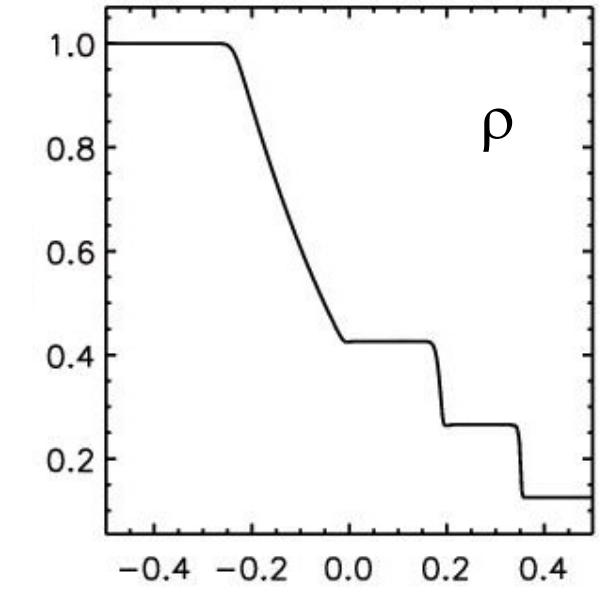


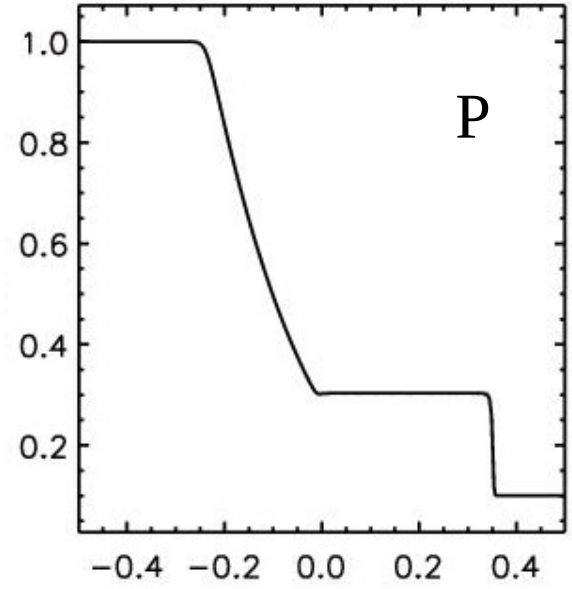


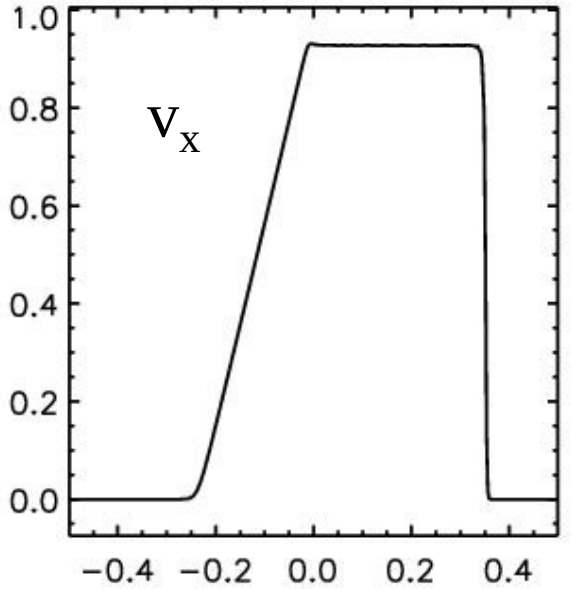


*Fig. 5.15a) left to right: density, pressure and x-velocity for RP with right-going shock and left-going rarefaction*

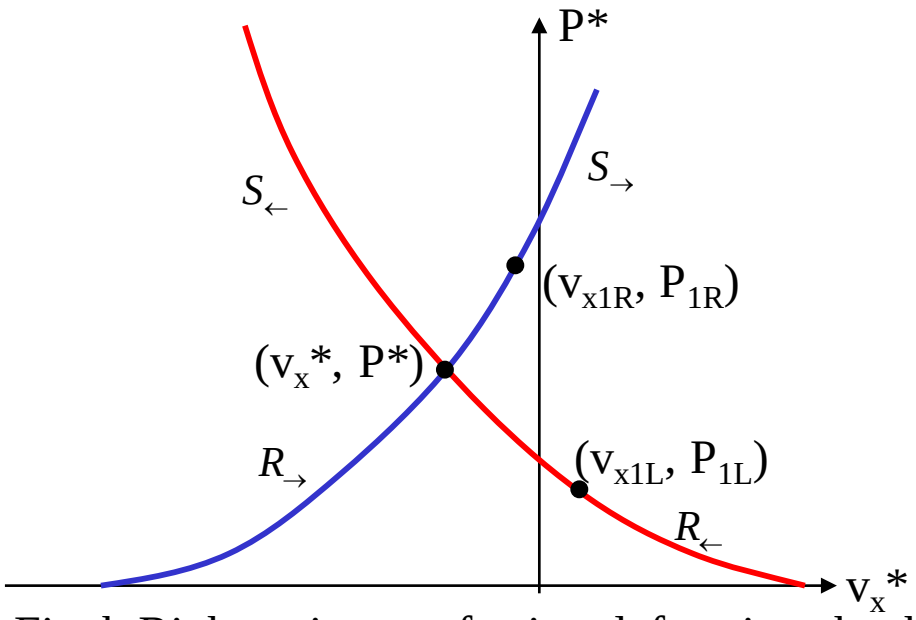


Fig. b Right-going rarefaction, left-going shock

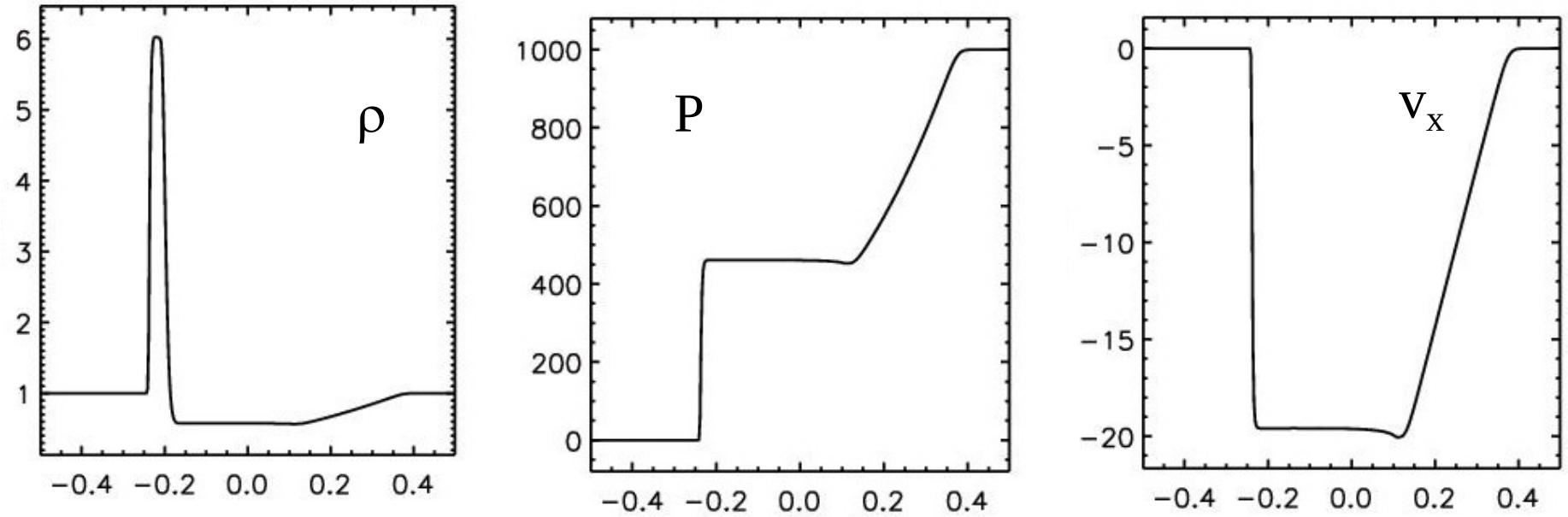


*Fig. 5.15b) left to right: density, pressure and x-velocity for RP with left-going shock and right-going rarefaction*

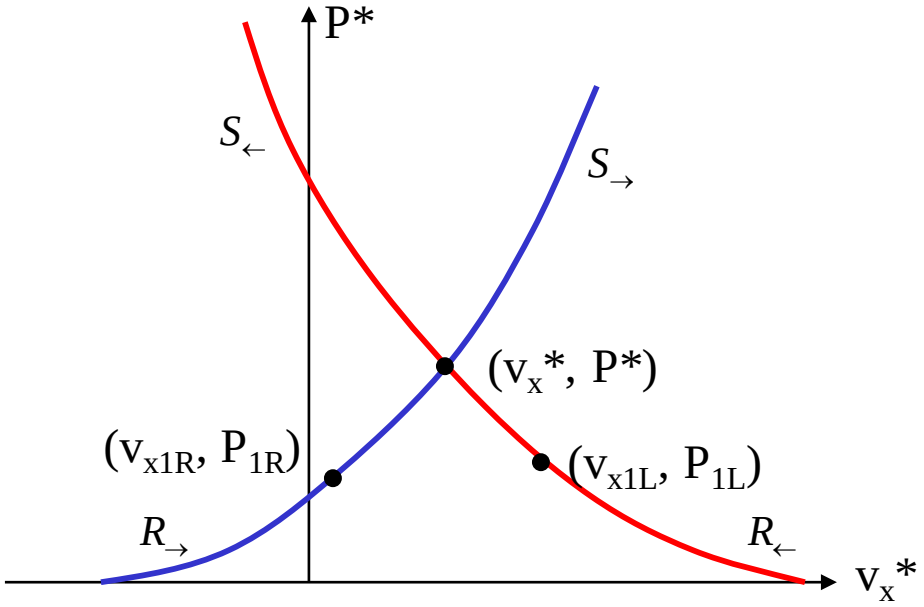


Fig. c Right-going shock, left-going shock

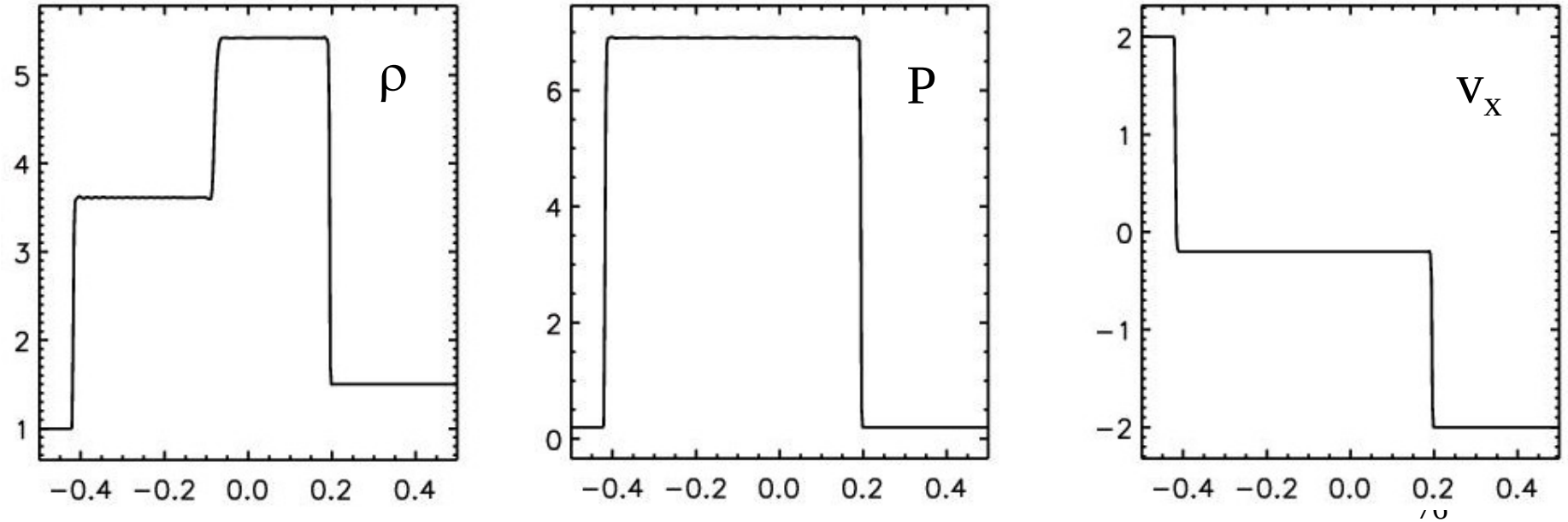


*Fig. 5.16a) left to right: density, pressure and x-velocity for RP with right- and left-going shocks*

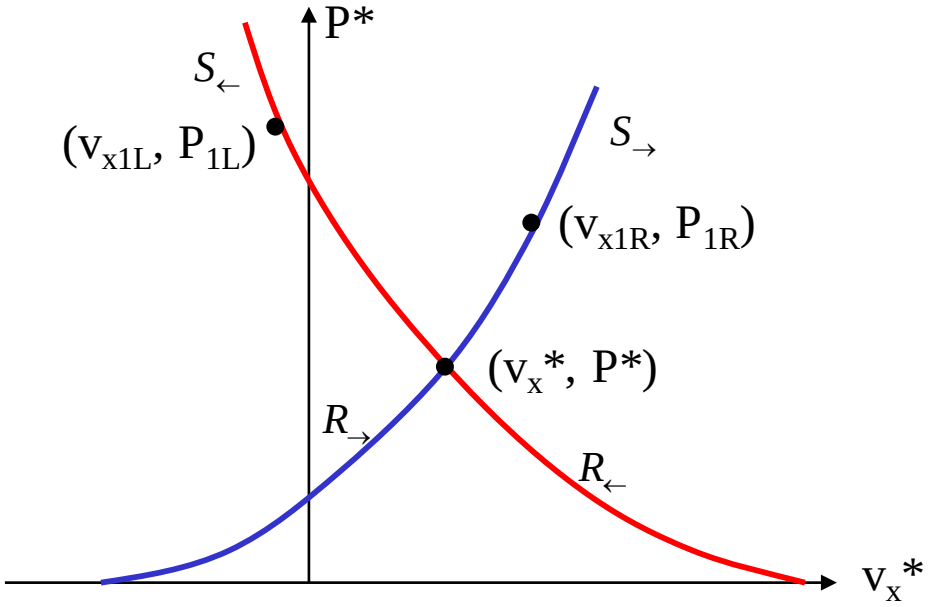


Fig. d Right-going rarefaction, left-going rarefaction

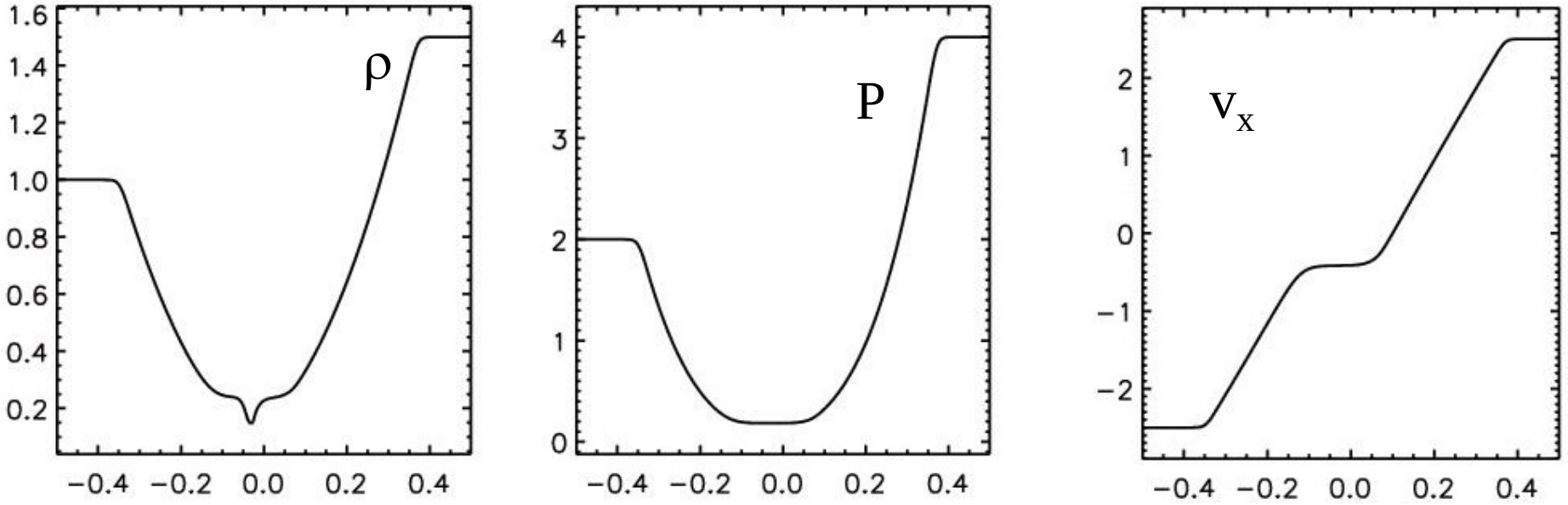


*Fig. 5.16b) left to right: density, pressure and x-velocity for RP with right- and left-going rarefaction fans*

Sketch of Solution Methodology : Recall our convention that "2" denotes post-shock or post-rarefaction fan quantities.

Let $\left(v^*_{x2R},\ P^*_{2R}\right)$ denote the *right - going* shock or *rarefaction fan* variables that connect to the initial right state $\left(v_{x1R},\ P_{1R}\right)$.

Similarly, let $\left(v^*_{x2L},\ P^*_{2L}\right)$ denote the *left - going* shock or *rarefaction fan* variables that connect to the initial left state $\left(v_{x1L},\ P_{1L}\right)$.

Our Job: Find the intermediate pressure $P^* = P^*_{x2L} = P^*_{x2R}$ for which $v^*_{x2L} = v^*_{x2R} = v^*_x$.

The Hard Part: The curves for right and left-going waves are highly non-linear so we have to *stably* iterate the *intermediate state* $\left(v^*_x, P^*\right)$ to convergence. Resolved state yields *numerical flux*.

The Trick: Replace rarefaction wave adiabats by rarefaction shocks. BUT be sure to enforce an *entropy fix*.

# 5.4.2) Numerical Solution of the Riemann Problem

Task: Given left state $\left(v_{x1L},\ P_{1L}\right)$ and right state $\left(v_{x1R},\ P_{1R}\right)$, find the intermediate state $\left(v_x^*,\ P^*\right)$.

For a *right-going shock* we can write:

$$v_{x2R}^* = v_{x1R} + \left(P^* - P_{1R}\right)/W_R\left(P^*\right)$$

where $W_R\left(P^*\right)$ has units of a shock speed in Lagrangian, i.e. mass, coordinates

$$W_R\left(P^*\right) = \sqrt{\left[\left(\Gamma-1\right)P_{1R} + \left(\Gamma+1\right)P^*\right]\rho_{1R}/2} \quad \text{for } P^* \geq P_{1R}$$

We can either analytically extend this expression for $P^* \geq P_{1R}$, which yields the *two-shock approximation*, or we can use the rarefaction fan solution for $P^* < P_{1R}$.

For a *left-going shock* we can write:

$$v_{x2L}^* = v_{x1L} - \left(P^* - P_{1L}\right)/W_L\left(P^*\right) \text{ with } W_L\left(P^*\right) = \sqrt{\left[\left(\Gamma-1\right)P_{1L} + \left(\Gamma+1\right)P^*\right]\rho_{1L}/2}$$

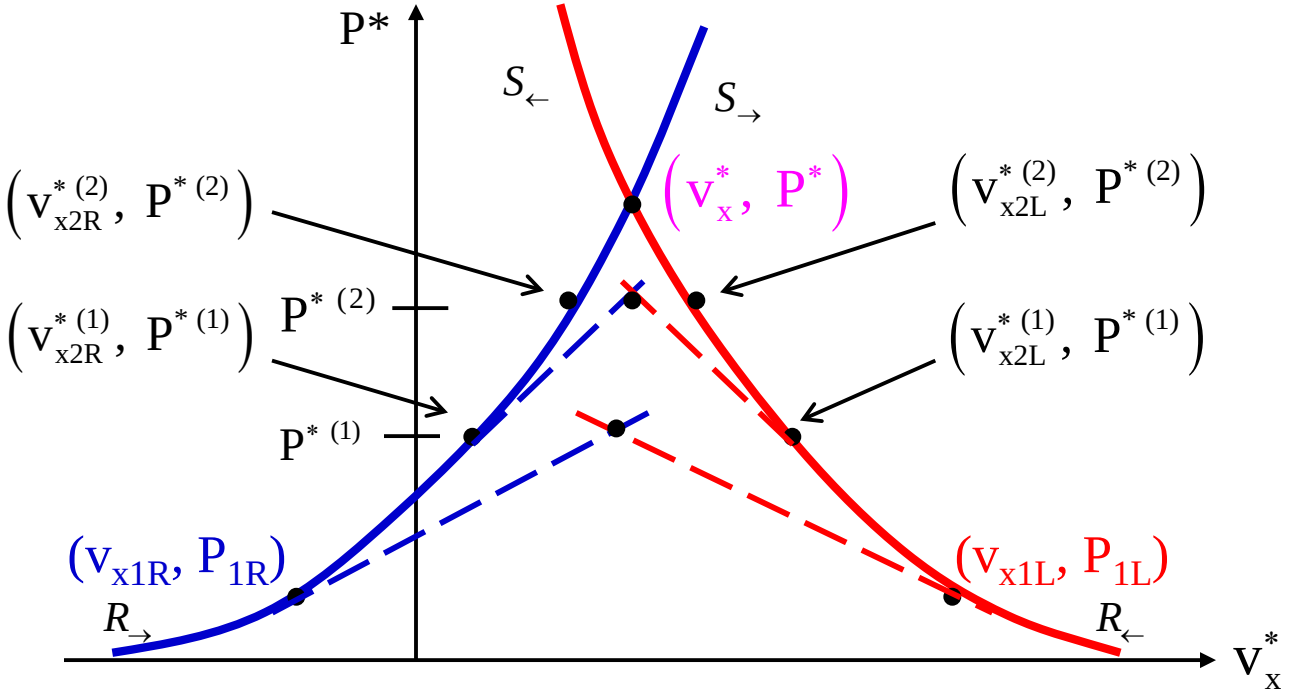


*Fig. 5.17 shows the first two iterations in the convergence of the Newton-Raphson based root solver for the Riemann problem. The adiabats associated with the right-going and left-going shocks are shown by the blue and red curves. The blue and red lines show the tangents to the corresponding curves. The point of intersection of the blue and red lines at each iteration yield the pressure that is used for the next iteration.*

Solution of the Riemann problem $\Leftrightarrow$

We have to find $P^*$ such that $v^*_{x2L} = v^*_{x2R} = v^*_x \quad \Leftrightarrow$

$$v_{x1L} - \left(P^* - P_{1L}\right)\Big/ W_L\left(P^*\right) = v^*_{x2L} = v^*_{x2R} = v_{x1R} + \left(P^* - P_{1R}\right)\Big/ W_R\left(P^*\right)$$

Question: But how do we start the iteration?

Answer: Set $W_L\left(P^*\right) \to W_L\left(P_{1L}\right)$ and $W_R\left(P^*\right) \to W_R\left(P_{1R}\right)$ to get:

$$P^{*(1)} = \frac{P_{1L}\, W_R\left(P_{1R}\right) + P_{1R}\, W_L\left(P_{1L}\right) - \left(v_{x1R} - v_{x1L}\right) W_R\left(P_{1R}\right) W_L\left(P_{1L}\right)}{W_R\left(P_{1R}\right) + W_L\left(P_{1L}\right)}$$

For very weak shocks, this may be all we need. In general, more is needed.

Using $n^{th}$ iterate $P^{*(n)}$, we can obtain $v^{*(n)}_{x2L}$ and $v^{*(n)}_{x2R}$ as follows:

$$v^{*(n)}_{x2L} = v_{x1L} - \left(P^{*(n)} - P_{1L}\right)\Big/ W_L\left(P^{*(n)}\right) ; \; v^{*(n)}_{x2R} = v_{x1R} + \left(P^{*(n)} - P_{1R}\right)\Big/ W_R\left(P^{*(n)}\right)$$

If we are far from convergence, we will not get $v^{*(n)}_{x2L} \approx v^{*(n)}_{x2R} \Rightarrow$ iterate further!

The *Newton - Raphson step* is designed to drive $v_{x2R}^{*(n)} - v_{x2L}^{*(n)}$ to zero:

$$0 = v_{x2R}^{*(n)} - v_{x2L}^{*(n)} + \left(P^{*(n+1)} - P^{*(n)}\right)\left(\frac{d\, v_{x2R}^{*(n)}}{d\, P^{*(n)}} - \frac{d\, v_{x2L}^{*(n)}}{d\, P^{*(n)}}\right)$$

Analytical expressions for the derivatives above are easily obtained:

For example:

$$1\Big/\left(\frac{d\, v_{x2R}^{*(n)}}{d\, P^{*(n)}}\right) \equiv Z_R\left(P^{*(n)}\right) = \frac{2\, W_R \left(P^{*(n)}\right)^3}{W_R \left(P^{*(n)}\right)^2 + \left(\rho_{1R}\ c_{s1R}\right)^2}$$

Further expressions are derived in the text. We can now obtain:

$$P^{*(n+1)} = P^{*(n)} - \frac{Z_R\left(P^{*(n)}\right) Z_L\left(P^{*(n)}\right)}{Z_R\left(P^{*(n)}\right) + Z_L\left(P^{*(n)}\right)} \left(v_{x2R}^{*(n)} - v_{x2L}^{*(n)}\right)$$



*In practice, only two or three iterations are needed* !